1982

Studies of molybdenum-molybdenum bonded species: 1. Synthesis and characterization of a reduction product of Cs3Mo2Cl8H; 2. Mixed sulfur chlorine substituted hexanuclear molybdenum clusters

Matthew Hermes Luly
Iowa State University

Luly, Matthew Hermes

STUDIES OF MOLYBDENUM-MOLYBDENUM BONDED SPECIES. 1. SYNTHESIS AND CHARACTERIZATION OF A REDUCTION PRODUCT OF CESIUM(3)MOLYBDENUM(2)CHLORIDE(8)HYDROGEN. 2. MIXED SULFUR CHLORINE SUBSTITUTED HEXANUCLEAR MOLYBDENUM CLUSTERS

Iowa State University PH.D. 1982

Studies of molybdenum-molybdenum bonded species. 1. Synthesis and characterization of a reduction product of $Cs_3Mo_2Cl_8H$. 2. Mixed sulfur chlorine substituted hexanuclear molybdenum clusters

by

Matthew Hermes Luly

A Dissertation Submitted to the
Graduate Faculty in Partial Fulfillment of the
Requirements for the Degree of
DOCTOR OF PHILOSOPHY

Department: Chemistry
Major: Inorganic Chemistry

Approved:

Signature was redacted for privacy.

In Charge of Major Work

Signature was redacted for privacy.

For the Major Department

Signature was redacted for privacy.

For the Graduate College

Iowa State University
Ames, Iowa

1982

TABLE OF CONTENTS

LIST OF FIGURES

LIST OF TABLES

FOREWORD

This dissertation deals with two distinct projects: a reduction product of $Cs_3Mo_2Cl_8H$ and a series of $(Mo_6S_{8-x}Cl_x)L_6$ (x = 0, 1, ..., 7) compounds. These studies are broadly related in that both of them deal with low-valent molybdenum species and metal-metal bonds are present in either the starting materials or products. Due to the divergent nature of these studies, they are treated independently. The reaction of $Cs_3Mo_2Cl_8H$ and zinc in pyridine was undertaken to elucidate the analogous reaction between Cs_3MoWCl_8H, a mixed-metal species, and zinc in pyridine. Eventually this project could no longer be profitably continued and was abandoned.

The reaction of Mo_6Cl_{12} with various sulfur-containing reagents was studied in order to find a new synthesis of Mo_6S_8 type compounds. The products formed by this approach are of the series $(Mo_6S_{8-x}Cl_x)L_6$ (x = 0, 1, ..., 7). The characterization of these materials is discussed in detail.

PART I. SYNTHESIS AND CHARACTERIZATION OF A REDUCTION PRODUCT OF $Cs_3Mo_2Cl_8H$

INTRODUCTION

The current surge of interest in metal-metal bonds has its origin in several different disciplines. Inorganic chemists have undertaken the systematic synthesis and structural characterization of dimers and larger metal clusters containing metal-metal bonds;[1,2,3] quadruply-bonded metal dimers with metal-metal distances as short as 1.828Å and well-formed clusters as large as $Pt_{15}(CO)_{30}^{2-}$ have been made.[4,5] This area of chemistry is obviously wide in scope and rich in potential. Metal clusters have been proposed and debated as possible models for chemisorbed species in heterogeneous catalysis.[6,7,8,9] If this proposal is even approximately correct, the understanding of surface chemistry in heterogeneous catalysis will be vastly enlarged. The electronic and stereochemical flexibility may make it possible to tailor metal clusters into highly selective homogeneous catalysts. The physical properties of some clusters, such as the superconductivity of the Chevrel phases,[10,11] have created both theoretical and experimental activity. Regardless of the future realization of their scientific and technological potential, metal-metal bonded dimers and clusters will greatly enrich the disciplines which study them.

Paralleling the increased study of metal-metal bonds

has been the growth of instrumental and computational techniques. In addition to the continual refinement of x-ray diffraction and established spectroscopic techniques,[12] there has been a host of more recent methods[6,13] which can be profitably applied to the characterization of metal dimers and clusters: Auger electron spectroscopy, x-ray photoelectron spectroscopy, ultraviolet photoelectron spectroscopy, secondary ion mass spectroscopy, low energy electron diffraction, acoustical spectroscopy, extended x-ray absorption fine structure spectroscopy and others. Some of these methods are surface techniques but can nevertheless be beneficially used in many cases to learn about metal-metal bonding and the bonding of species adsorbed to surface atoms. The acquiescence of theoreticians to investigate the complex problems posed by the electronic structure of dimers and clusters has also assisted in the understanding of metal-metal bonds.[14,15,16]

Metal dimers provide the simplest examples of metal-metal bonds. It was the realization in 1964 that $K_2Re_2Cl_8$ contained a rhenium-rhenium quadruple bond which provoked much of the subsequent work on metal-metal bonded dimers.[17] Russian workers published the structure of "$(C_5H_5NH)HReCl_4$" which they claimed to be a dimer with four bridging hydrogen atoms.[18] The bridging hydrogens were necessary in their

view to account for the observed rhenium oxidation state of 2+. Shortly thereafter, a determination of the crystal structure of $KReCl_4 \cdot 2H_2O$ showed a Re_2Cl_8 unit nearly identical to that in "$(C_5H_5NH)HReCl_4$": an almost cubic array of chlorine atoms containing a pair of rhenium atoms nearly centered on opposite faces with a metal-metal separation of 2.24Å.[19] Subsequent work on "$(C_5H_5NH)HReCl_4$" led to an oxidation state of 2.9+ for rhenium and the originally proposed hydrogens appear to be specious.[20] The metal-metal bonding in $Re_2Cl_8^{2-}$ consists of one σ, two π, and a δ component: the now well-known quadruple bond. If the Re-Re axis is considered to be the z axis and the Re-Cl bonds are taken as the x and y axes, the $d_{x^2-y^2}$, s, p_x and p_y orbitals of each metal atom form the Re-Cl bonds. The d_{z^2} orbitals form the σ bond, the d_{yz} and d_{xz} orbitals form the two π bonds and the δ bond arises from the d_{xy} orbitals. The eclipsed configuration of the chlorine atoms is a manifestation of the δ bond: the δ overlap is maximized by an eclipsed configuration. The short Re-Re bond distance is due to the manifold nature of the bond. All of the work on metal-metal bonded dimers of high bond order can be traced to this discovery.

Today an enormous body of literature concerning dimers with metal-metal multiple bonds exists.[16,21,22,23] Dimers

with bond orders as high as four are common and the existence of Nb_2 in inert gas matrices as well as Mo_2 in both inert gas matrices and the gas phase suggests the formation of pentuple and sextuple bonds, respectively.[24,25,26,27] Quadruple bonds are currently known to be formed by chromium, molybdenum, tungsten, technetium and rhenium. Such bonds have provided two of the more interesting problems arising from dimers: the large dispersion of Cr-Cr quadruple bond lengths and the reluctance of tungsten to enter into quadruple bonds.

Authors are fond of observing that 126 years elapsed between the synthesis of $Cr_2(O_2CCH_3)_4(H_2O)_2$ and the realization that it contained a quadruple bond.[16,21,23,28,29] The known Cr-Cr quadruple bonds range from 1.828Å in Cr_2(5-methyl-2-methoxyphenyl)$_4$ to 2.541Å in $Cr_2(O_2CCF_3)_4(C_2H_5OC_2H_5)_2$ (the known Mo-Mo quadruple bonds are encompassed by 2.037Å to 2.183Å).[30] The longer bond distances appear chiefly in the compounds $Cr_2(O_2CR)_4 \cdot 2L$ and the assignment of a quadruple bond to compounds in this class created a controversy. An early calculation claimed a $\sigma^2 \delta^2 \hat{\delta}^{*2} \sigma^{*2}$ configuration with no net bonding between the chromium atoms in $Cr_2(O_2CH)_4 \cdot 2H_2O$.[31] Extensive synthetic, structural and computational work has since provided a comprehensive explanation of the bond distance latitude.[30,32] Most quad-

ruply bonded chromium dimers belong to one of two groups: (1) $Cr_2(O_2CR)_4 \cdot 2L$ compounds where L is a solvent molecule or an axial O-Cr interaction between adjacent dimers in the solid state which have intramolecular Cr-Cr distances between 2.283 and 2.541Å; (2) Compounds with Cr-Cr distances less than 1.90Å, dubbed "supershort" bonds, where the ligands are usually derived from weak acids and frequently have the axial ligand positions blocked by intramolecular steric hindrance. By choosing ligands carefully, a molecule can be designed to fit either of the above categories. It has been observed that the Cr-Cr distance increases as the number of axial ligands increases.[30,32] In one series of dimers, the addition of one axial ligand to a compound increased the metal-metal distance 0.15Å over the compound lacking axial ligands. The addition of two axial ligands increased the metal-metal distance an additional 0.23Å over the compound with one axial ligand. Also evident is an increase in Cr-Cr distance with an increase in terminal ligand basicity. Another factor is the donor strength of the bridging ligand with the strongest donors having the shortest Cr-Cr distances. The donor strength of the bridging ligands is primarily a function of the atoms bonded to the metal atoms. Acidity for these atoms decreases in the order OH>NH>CH so the donor strengths of the corresponding anions increase in the order $O^- < N^- < C^-$. The chromium dimers provide a probe to investigate

the factors affecting metal-metal quadruple bonds not found in dimers of other elements.

Tungsten-tungsten quadruple bonds have also aroused much interest. The discovery of a quadruply bonded tungsten species is a recent one. Over ten years passed from the discovery of the first molybdenum quadruply bonded dimer[33] until the discovery of the first quadruply bonded tungsten species. The elusive tungsten quadruple bond, first found in $MoW(O_2CC(CH_3)_3)_4$, was reported in 1976.[34] The first W-W quadruple bond was reported a year later in the $W_2(CH_3)_{8-x}Cl_x^{4-}$ anion.[35] Currently, a number of quadruply bonded tungsten dimers are known.[23,36]

While investigating the chemistry of the molybdenum-tungsten bimetallic compounds, it was determined that the $MoWCl_8H^{3-}$ ion could be prepared.[37] This ion, depicted in Figure 1, is isostructural with the previously known dimolybdenum $Mo_2Cl_8H^{3-}$ ion.[38,39,40] The metal positions in $MoWCl_8H^{3-}$ are disordered and occupied with equal probability by either molybdenum or tungsten. The Mo-W triple bond in Cs_3MoWCl_8H is 2.445(3)Å while the Mo-Mo triple bond in $Rb_3Mo_2Cl_8H$ is 2.38(1)Å. In addition to the difference in bond lengths, differences in reactivity also exist.[41] The attempt to prepare the heteronuclear analogue of $Mo_2Cl_4(C_5H_5N)_4$ demonstrates that the reactivity of $MoWCl_8H^{3-}$ is much different than the reactivity of $Mo_2Cl_8H^{3-}$. After refluxing

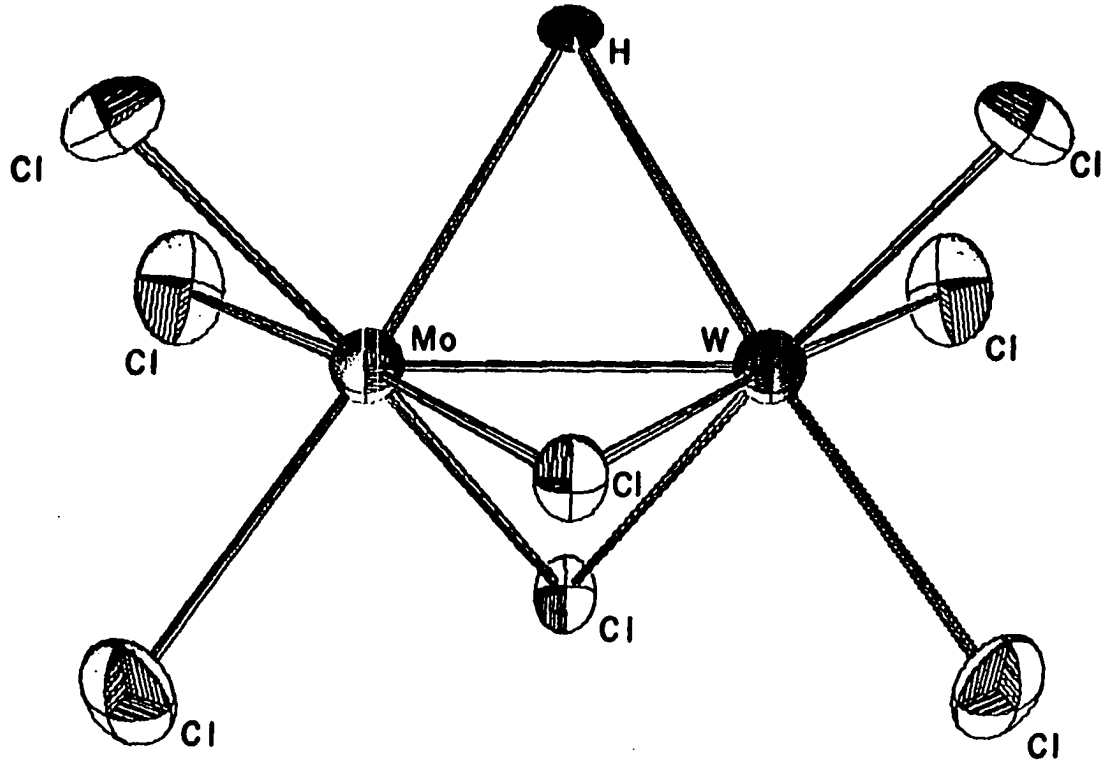

Figure 1. Structure of $MoWCl_8H^{3-}$ ion

$Cs_3Mo_2Cl_8H$ in pyridine for a few hours, red crystals of $Mo_2Cl_4(C_5H_5N)_4$ precipitate.[42] No reaction occurs when Cs_3MoWCl_8H is refluxed in pyridine, but when the reaction is executed in the presence of zinc a black solution results. Black crystals can be isolated from this reaction and the crystals are known from single crystal x-ray diffraction to be $ZnCl_2 \cdot 2(C_5H_5N)$.[41] Apparently, enough of a molybdenum impurity species is present to impart a black color to the usually white $ZnCl_2 \cdot 2(C_5H_5N)$. It is also known that the reaction of $Cs_3Mo_2Cl_8H$ and zinc in refluxing pyridine gives rise to a black solution, and ultimately black crystals similar in appearance and properties to the mixed metal product. It is the homonuclear reduction product which will be the subject of this dissertation.

The original purpose of this work was to identify and characterize the black material resulting from the zinc reduction of Cs_3MoWCl_8H. As the mixed metal starting compound is difficult to prepare,[37] the analogous product from the more easily synthesized $Cs_3Mo_2Cl_8H$ was prosecuted first. This was to be just one step in the comprehensive exploration of the chemistry of di-nuclear mixed-metal compounds in particular, and dimers and larger clusters in general. However, the obdurate black product is not easily characterized and the scope of the work became a multitechnique attempt to characterize an anomalous material. This work is an example

of a comprehensive study in which both routine and highly sophisticated methods of analysis fail to unambiguously identify a material. The study offers an interesting view of some strengths and limitations of current methods of analysis.

EXPERIMENTAL METHODS

All chemicals, except solvents, were generally used without further purification. ACS grade pyridine was dried by standing over phosphorous pentoxide, vacuum distilled onto dried, degassed 4A molecular sieves and vacuum distilled as necessary. ACS grade benzene and acetonitrile were dried and degassed according to the literature,[43] stored over dried, degassed 3A molecular sieves and vacuum distilled as required.

The oxygen and water sensitivity of many of the compounds used often dictated the use of inert atmosphere techniques. When necessary, reactions and filtrations were done under an atmosphere of pre-purified nitrogen in specially designed glassware. Solvents were distilled on a vacuum line (ca. 10^{-4} Torr) or syringed into the receiving flask under a nitrogen flow. Air sensitive solids were handled in a dry box containing an atmosphere of pre-purified nitrogen which was circulated through 4A molecular sieves to remove water and Chemalog catalyst R3-11 to remove oxygen. The dew point of this dry box was typically -75°C.

Carbon, hydrogen, nitrogen and zinc analyses were performed by the Ames Laboratory Analytical Services Group. Molybdenum was determined gravimetrically by the 8-hydroxyquinoline method[44] after decomposition of the sample in hot, basic peroxide solution. Chlorine samples were decomposed in

hot, basic peroxide solutions, acidified to a pH of 3 to 5, and potentiometrically titrated with standard $AgNO_3$. Oxidation states were determined chemically. Weighed samples were dissolved in an excess of a standard acidic cerium (IV) solution; excess Ce^{4+} was then titrated with standard Fe^{2+} solution. The apparent oxidation state of the molybdenum is then given by 6.0 - ((moles Ce^{4+} - moles Fe^{2+})/(moles Mo)).

Routine infrared spectra in the region 4000 to 200 cm^{-1} were run as nujol mulls between cesium iodide plates on a Beckman IR 4250 spectrometer. Band positions in the spectra are considered accurate to ± 2 cm^{-1}. Ultraviolet and visible spectra were obtained using a Cary Model 14 spectrometer.

X-ray diffraction powder patterns were obtained using a 114.6 mm radius Debye-Scherrer camera. Samples were packed in 0.3 mm Lindemann thin-walled glass capillaries, sealed under nitrogen and exposed to filtered copper x-rays for 16 to 24 hours. All electron microscopy was done using a JEOL 100cx instrument. Samples were loaded into the instrument by means of a glove bag attached to the port.

Room temperature electron paramagnetic resonance spectra were obtained with a Varian E-4 spectrometer. Low temperature spectra were obtained with a Bruker ER220 spectrometer. Powders were run in evacuated, sealed 5 mm OD pyrex or quartz tubes, and solutions were run in a quartz cell designed for air sensitive liquids. Spectra were calibrated with DPPH.

Combined rotation and multiple pulse NMR spectroscopy (CRAMPS) were obtained using a locally built instrument.[45] The samples were contained in rotors which were modified to protect air sensitive samples.

X-ray photoelectron spectra were run on an AEI Model ES200B spectrometer. Monochromatic Al K_α radiation (1486.6 eV) was used, and when necessary, an electron flood gun was employed to reduce the effects of sample charging. While in a dry box, powdered samples were pressed onto the surface of a strip of silver-cadmium alloy or indium, and loaded directly from the dry box into the connecting spectrometer. Spectra were referenced to the 285.0 eV carbon peak and interpreted with the computer program APES[46] (see Appendix).

All electrochemistry was done using a Princeton Applied Research Model 175 Universal Programmer, Model 179 Digital Coulometer, Model 173 Potentiostat/Galvanostat, Model 178 Electrometer Probe and platinum electrodes. The samples were dissolved in a 0.2M Bu_4NBF_4 pyridine solution.

$Mo_2(CH_3COO)_4$[34] and $Cs_3Mo_2Cl_8H$[40] were prepared according to literature methods. $Mo_{1.0}Cl_{0.6}(C_5H_5N)_{1.2}$ was prepared by refluxing 10.82 g (12.4 mmole) of $Cs_3Mo_2Cl_8H$ and 7.22 g (110.4 mmole) of zinc powder in about 120 mL of dry, deoxygenated pyridine, under nitrogen, for 83 hours. The black solution was filtered to remove CsCl and unreacted zinc, and the pyridine was pumped off by vacuum. The resulting black

solid was ground to a powder and extracted continuously with benzene for 6 weeks to remove $ZnCl_2 \cdot 2(C_5H_5N)$. If instead of being extracted with benzene, the black solid was washed briefly three times with deoxygenated concentrated hydrochloric acid, $MoCl_{1.1}(C_5H_5N)_{0.8}$ was obtained. $MoCl_{1.1}(C_5H_5N)_{0.8}$ could also be made by refluxing 4.70 g (7.23 mmole) of $Mo_2Cl_4(C_5H_5N)_4$ with 3.34 g (51.09 mmole) of zinc in ca. 50 mL of dry, degassed pyridine for 85 hours, filtering and washing with acid. Table I lists the analytical results of the more thoroughly characterized acid washed products.

Table I. Summary of analytical data

Formula[a]	% Mo	% Cl	% C	% H	% N	% Zn	Oxidation State
$Mo_{1.0}Cl_{1.1}(C_{5.0}H_{5.7}N_{1.0})_{0.8}$	44.16	18.18	22.73	2.16	5.38	-	0.5+
-	-	-	22.47	2.16	5.44	1.08	-
$Mo_{1.0}Cl_{1.1}(C_{5.0}H_{5.4}N_{1.0})_{0.9}$	45.25	18.52	24.13	2.20	5.85	-	0.5+
$Mo_{1.0}Cl_{x}(C_{5.0}H_{5.1}N_{1.0})_{0.9}$	46.31	-	25.22	2.16	6.02	-	0.1+
$Mo_{1.0}Cl_{1.0}(C_{5.0}H_{5.2}N_{1.0})_{0.8}$[b]	46.05	17.62	24.50	2.12	5.90	-	0.1+
$Mo_{1.0}Cl_{x}(C_{5.0}H_{4.9}N_{1.0})_{0.8}$[c]	46.48	-	22.80	1.88	5.42	1.92	0.4+
$Mo_{1.0}Cl_{1.0}(C_{5.0}H_{4.6}N_{1.0})_{0.8}$[d]	48.24	17.67	24.45	1.88	5.79	-	0.0

[a]Formulas are based on ratios of elements exhibited by analyses. Unless otherwise noted all entries are acid washed products of the reaction of $Cs_3Mo_2Cl_8H$ and zinc in pyridine.

[b]$Mo_2Cl_4(C_5H_5N)_4$ was used as starting material instead of $Cs_3Mo_2Cl_8H$.

[c]Sample prepared by heating $Mo_{1.0}Cl_{1.1}(C_{5.0}H_{5.7}N_{1.0})_{0.8}$ in a dynamic vacuum at 210°C overnight.

[d]Sample prepared by heating $Mo_{1.0}Cl_{1.0}(C_{5.0}H_{5.2}N_{1.0})_{0.9}$ in a dynamic vacuum at 300°C for one day.

Table I. (continued)

Formula	% Mo	% Cl	% C	% H	% N	% Zn	Oxidation State
$Mo_{1.0}Cl_{0.7}C_{3.7}H_{1.7}N_{0.8}$[e]	52.82	13.90	24.18	0.92	6.07	-	-
$Mo_{1.0}Cl_{0.7}(C_5H_5N)_{0.7}(C_2H_3O_2)_{0.5}$[f]	43.04	11.76	25.78	2.35	4.68	-	-

[e]Sample prepared by heating $Mo_{1.0}Cl_{1.1}(C_{5.0}H_{5.7}N_{1.0})_{0.8}$ in a dynamic vacuum at 425°C for 63 hours.

[f]Sample prepared by refluxing $Mo_{1.0}Cl_{1.0}(C_{5.0}H_{5.2}N_{1.0})_{0.8}$ in acetic acid for two days.

CHARACTERIZATION OF REDUCTION PRODUCT

Once it was known that the black solid obtained from the reduction of $Cs_3Mo_2Cl_8H$ with zinc in pyridine contained substantial amounts of $ZnCl_2 \cdot 2py$ (py = pyridine), the separation of $ZnCl_2 \cdot 2py$ was prosecuted. The black material and the zinc impurity species have extremely similar solubilities in pyridine. Attempts to separate them by solvent extraction were only successful in benzene in which the $ZnCl_2 \cdot 2py$ was slightly soluble and the black material was insoluble. After prolonged extraction with benzene the black substance approached the composition $Mo_{1.0}Cl_{0.6}py_{1.2}$. The resulting solid showed coordinated pyridine and chlorine in the infrared spectrum (Table II) and was amorphous to x-rays as evidenced by the absence of a powder pattern. The disadvantage of a benzene extraction was that it required approximately two months for completion.

Further research demonstrated that brief washing with concentrated hydrochloric acid successfully effected the separation of $ZnCl_2 \cdot 2py$. The black solid thus obtained had the advantage of relative ease of preparation although it had a significantly different stoichiometry (typically $Mo_{1.0}Cl_{1.1}py_{0.8}$) than the benzene washed material. Only the acid washed materials will be discussed further. The properties of the acid washed materials are somewhat sample dependent. Except when noted, the physical characteristics are quite

Table II. Summary of selected infrared frequencies[a]

A[b]	B[c]	C[d]	D[e]	E[f]	F[g]	G[h]
						1748m
						1712m
1600m	1590s,b	1601s	1591s,b	1588s,b		1599m
		1560vw	1560vw			
	1525m,b					1518m
		1484m				
1465s	1458s	1460s	1460s	1455s	1460s	1441s,vb
		1447s				
1375s	1375s	1375s	1375s	1375s	1376s	1376m
1305w	1305w	1301w	1303vw	1303w		1310vw
						1290vw
			1259w			
1220w		1217s	1215w	1216w		1211w

[a]Spectra were run as mineral oil mulls on CsI plates.

[b]$Mo_{1.0}Cl_{0.6}py_{1.2}$ (benzene washed material).

[c]$Mo_{1.0}Cl_{1.1}py_{0.8}$ (acid washed material).

[d]$Mo_2Cl_4py_4$.

[e]$Mo_{1.0}Cl_xpy_{0.8}$ (prepared by heating to 210°C).

[f]$Mo_{1.0}Cl_{1.0}py_{0.8}$ (prepared by heating to 300°C).

[g]$Mo_{1.0}Cl_{0.7}C_{3.7}H_{1.7}N_{0.8}$ (prepared by heating to 425°C).

[h]$Mo_{1.0}Cl_{0.7}py_{0.7}(C_2H_3O_2)_{0.5}$ (prepared by refluxing in acetic acid).

Table II. (continued)

A	B	C	D	E	F	G
	1192w					
1158m	1155m	1145m	1153m	1152m		1151m
	1086w		1096w	1101w		1082m
1070m		1071m	1063w	1063w		
1045m	1045w	1039m	1039w	1042w		1039vw
1015w	1015w	1005m	1007w	1009w		1013w
945s,b		979w				
915w	885w	877m		865w		
	805w		799w	844w		
755m	765m	750s	755s	756s		760s
732s,b	742s					
	720m	716w	720w	723s	717w	
690m,b	666m	689s	691m	695w		670s
		668w	670vw			
		631w	634w			623m
			592vw		590vw	588w
					553vw	531w
		434w				
	415w	410vw			412w	
	392w	388w	390vw		390w	
		377vw				
		360w			360w	

Table II. (continued)

A	B	C	D	E	F	G
315w,b	319s,b	338s	316s,b		341m,b	
		270w				256s,b

similar and $Mo_{1.0}Cl_{1.1}(C_{5.0}H_{5.7}N_{1.0})_{0.8}$ (referred to as $Mo_{1.0}Cl_{1.1}py_{0.8}$) will be discussed as representative of these substances.

The stoichiometry of this material is quite unusual; elemental analysis pronounces it $Mo_{1.0}Cl_{1.1}py_{0.8}$. This formulation indicates an oxidation state of approximately 1+ for molybdenum — something uncommon, but certainly known.[47] Two simple explanations for the low ligand-to-metal ratio observed are the coexistence of molybdenum metal and a molybdenum, chlorine, pyridine compound or compounds; or the extensive use of bridging ligands possibly combined with extensive metal-metal bonding.

The chemically determined oxidation state of molybdenum, which is very sample dependent, does not clarify the matter. The oxidation state of the acid-washed materials typically falls in the range of 0.0 to 0.5+, with 0.5+ being representative. This is quite different than the approximately 1+ value indicated by the stoichiometry. An explanation of this anomalously low value is not obvious. Even if the small amount of zinc impurity were present as the metal (ca. 1%), it could not account for the observed result. A significant amount of elemental molybdenum metal present in the product could cause such a result, as would the presence of a hydride. Using the cerium-iron method of analysis, $Cs_3Mo_2Cl_8H$ has an apparent oxidation state of 2.5+ per

molybdenum instead of the true value of 3.0+ per molybdenum. This result undoubtedly arises from the presence of the hydride ligand. Similarly, if the molybdenum in $Mo_{1.0}Cl_{1.1}py_{0.8}H_x$ were truly Mo(II), the apparent oxidation state of 0.5+ could be explained by x = 3/2; a "true" Mo(III) would require x = 5/2 to explain the observed oxidation state, etc. The difficulty of this explanation is the irresolvable conflict between explaining the oxidation state and maintaining the electrical neutrality of the material. If the experimentally determined oxidation state is represented by E, the "true" oxidation state is represented by T, and x is the number of hydrides in $Mo_{1.0}Cl_{1.1}py_{0.8}H_x$ then electrical neutrality requires $T = 1.1 + x$. The experimental oxidation state data require $E = T - x = 0.5$. When these are rewritten as $T = 1.1 + x$ and $T = 0.5 + x$, it is clear that no solution exists which satisfies both equations. The meaning of this result is not clear but it may be that the hydride model is not the proper explanation, or at best is only partially correct. A similar analysis of $Cs_3Mo_2Cl_8H$ shows the two equations are identical.

Another difficulty of the hydride model is the absence of conclusive evidence of its presence. Frequently, the samples have $H/C > 1$, but in general there is only a small excess of hydrogen compared to that expected for pyridine alone and its significance is difficult to assess. Spectro-

scopic analyses are also ambiguous. However, the determination of hydrogen is frequently a difficult matter. Examples found in the literature are the delusive hydrogens proposed for some rhenium dimers[18,20] and the seven year hiatus of the discovery of the hydride in $Mo_2Cl_8H^{3-}$.[39,40]

The cyclic voltammogram for $Mo_{1.0}Cl_{1.1}py_{0.8}$ is shown in Figure 2. The irreversible reductions at -0.06, -0.76, and -1.76 volts and irreversible oxidations at +1.30 and +1.57 volts are not easily assigned. While the cyclic voltammogram does not perspicuate the experimental oxidation state determination, it is interesting that the compound does suffer reduction.

X-ray powder diffraction of $Mo_{1.0}Cl_{1.1}py_{0.8}$ proved it to be amorphous. Prior to this experiment, one explanation of the low ligand-to-metal ratio had been based upon the presence of molybdenum metal. As it is unlikely that the molybdenum metal which might be formed during the reaction would all be amorphous, the diffraction experiment seems to dictate against this possibility.

In an attempt to learn more about the morphology of the particles, electron microscopy was employed. Figures 3, 4, and 5 show scanning electron microscopy photographs. Particle size varies substantially as the method of preparation would indicate. Most particles fall in the range of 200 microns to less than 1 micron. The particles are irreg-

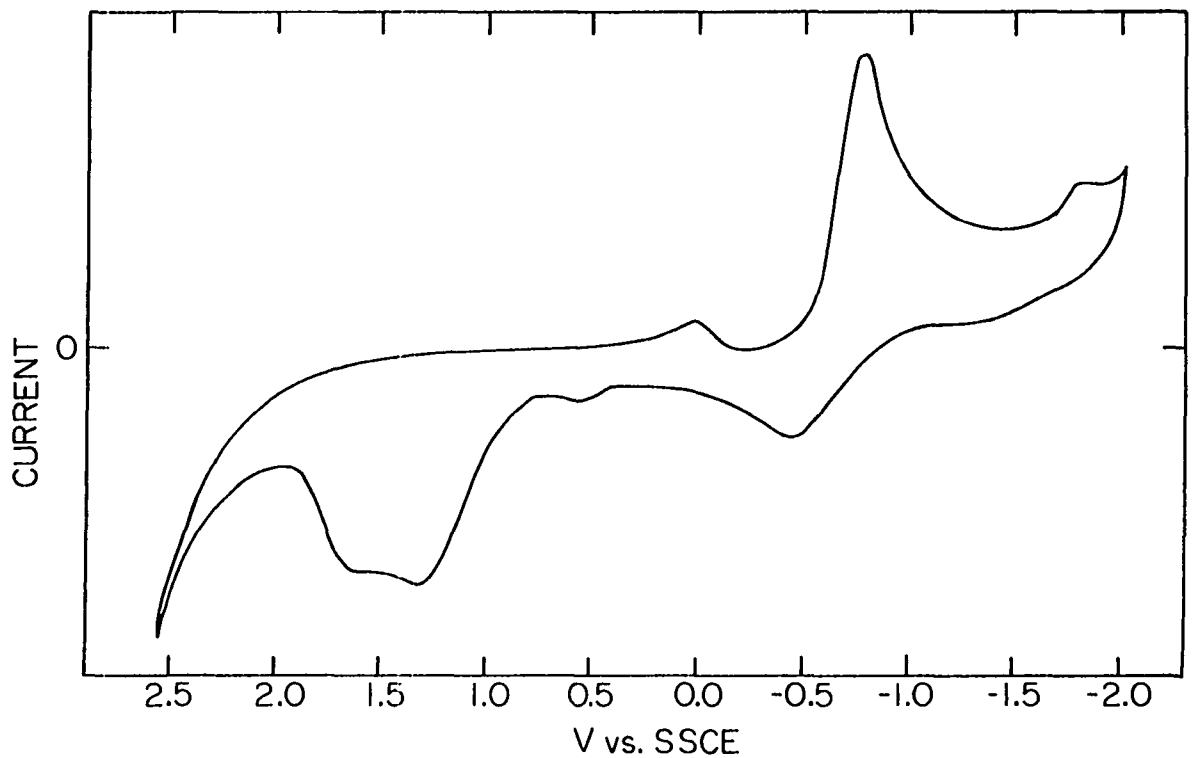

Figure 2. Cyclic voltammogram of $Mo_{1.0}Cl_{1.1}py_{0.8}$ in pyridine

Figure 3. Electron micrograph of $Mo_{1.0}Cl_{1.1}py_{0.8}$

Figure 4. Electron micrograph of $Mo_{1.0}Cl_{1.1}py_{0.8}$

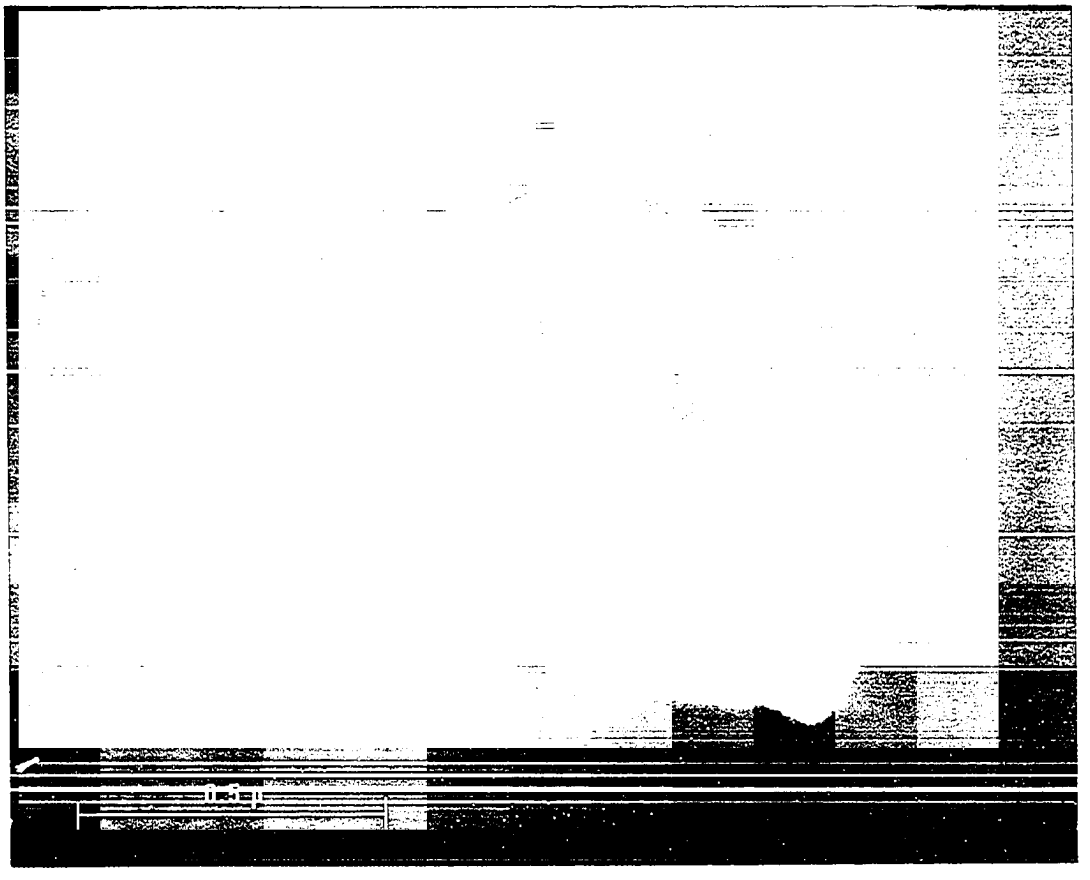

Figure 5. Electron micrograph of $Mo_{1.0}Cl_{1.1}py_{0.8}$

ularly shaped demonstrating little or no angularity which might indicate crystallinity. There is no evidence for a mixture of two or more distinct types of particles which could indicate that $Mo_{1.0}Cl_{1.1}py_{0.8}$ is a mixture of two or more materials. Finally, on a particulate scale, there is no evidence of electron diffraction, substantiating the amorphous character of the material.

The amorphousness of $Mo_{1.0}Cl_{1.1}py_{0.8}$ precludes an exact diffraction solution of its structure, but the structural implications of this property can be considered. The amorphous state is defined as the absence of long range order, although short range order is generally conceded. The random arrangement of misoriented microcrystallites has frequently been used to describe amorphous materials.[48] The amorphous state of organic polymers is attributed to various factors: the great length of chains, lack of stereoregularity, and random cross-linking of chains.[49] The absence of extended, three-dimensional order in $Mo_{1.0}Cl_{1.1}py_{0.8}$ could have several origins. $Mo_{1.0}Cl_{1.1}py_{0.8}$ could be discrete, well-defined clusters which pack randomly; the accretion of mono-nuclear species or clusters which are not well defined; or an extended polymer or array which is not regular and may be non-stoichiometric. This is speculation, but would seem to include the more plausible explanations of the amorphousness and empirical formula.

The infrared spectra of $Mo_{1.0}Cl_{1.1}py_{0.8}$ are of consistently poor quality (Table II), and as a result the useful information is limited. The pyridine is present as coordinated pyridine. There is a broad band (Mo-Cl or Mo-N) at 319 cm^{-1}. Weak bands at 1525 cm^{-1} and 1305 cm^{-1} are very similar to pyridinium bands (1540, 1327 cm^{-1}), yet the other pyridinium bands are missing (1640, 1540, 1327, 1295 and 1250 cm^{-1})[50] so this is not the correct interpretation. These two bands are similar to the 1553 cm^{-1} and 1248 cm^{-1} hydride bands in $Cs_3Mo_2Cl_8H$. Washing the crude product with concentrated DCl instead of HCl resulted in the disappearance of the 1525 cm^{-1} band, the 1305 cm^{-1} band being unchanged, and no appearance of bands near 1101 cm^{-1} and 904 cm^{-1}. This anomalous result does not resolve the hydride question. The 1525 cm^{-1} and 1305 cm^{-1} bands are also similar to the 1560 cm^{-1} and 1301 cm^{-1} bands seen in $Mo_2Cl_4py_4$. It would seem these two weak bands may be nothing more than coordinated pyridine or a small amount of impurity. Side reactions of the pyridine, such as dimerization or hydrogenation, would result in larger changes in the infrared spectrum.[51]

The visible and ultraviolet spectrum in pyridine has peaks at 6095, 5714, and 3200 Å. These are similar to bands seen in some dinuclear molybdenum (II) compounds; $Mo_2Cl_4py_4$ has peaks at 5730 Å and 6350 Å.

$Mo_{1.0}Cl_{1.1}py_{0.8}$ exhibits a rather featureless EPR spec-

trum having a g of 1.95. Figure 6 is a typical room temperature powder spectrum. The small peak at higher field is due to an oxidized impurity. Spectra run at 150°K were identical to room temperature spectra except for a slight sharpening of the peaks. Attempts to obtain a solution spectrum were fruitless. This may be due to saturation or insufficient sensitivity of the instrument.

Solid state NMR spectroscopy has the potential to solve the hydride ambiguity. A hydride, if it were present, would engender a peak in the proton NMR in addition to the pyridine proton peaks. If there were no hydride, only pyridine proton signals would be present. CRAMPS experiments pronounce all the protons in $Mo_2Cl_4py_4$ to be equivalent (5.3δ). Because the difference in chemical shifts of the pyridine hydrogens is small compared to their full-widths at half-maximum (FWHM's), a single symmetric peak is observed. The spectrum observed for $Cs_3Mo_2Cl_8H$ consists of a single, slightly asymmetric peak (0.2δ). The spectrum of $Mo_{1.0}Cl_{1.1}py_{0.8}$, shown in Figure 7, exhibits a definite shoulder. This could be construed as overlapping pyridine and hydride peaks. However, it is possible that effects similar to those causing the asymmetric peak in $Cs_3Mo_2Cl_8H$ are acting on the pyridine protons in $Mo_{1.0}Cl_{1.1}py_{0.8}$ to cause an asymmetric peak. The signal observed for material washed with concentrated DCl is quite similar in shape to the signal of the concentrated HCl

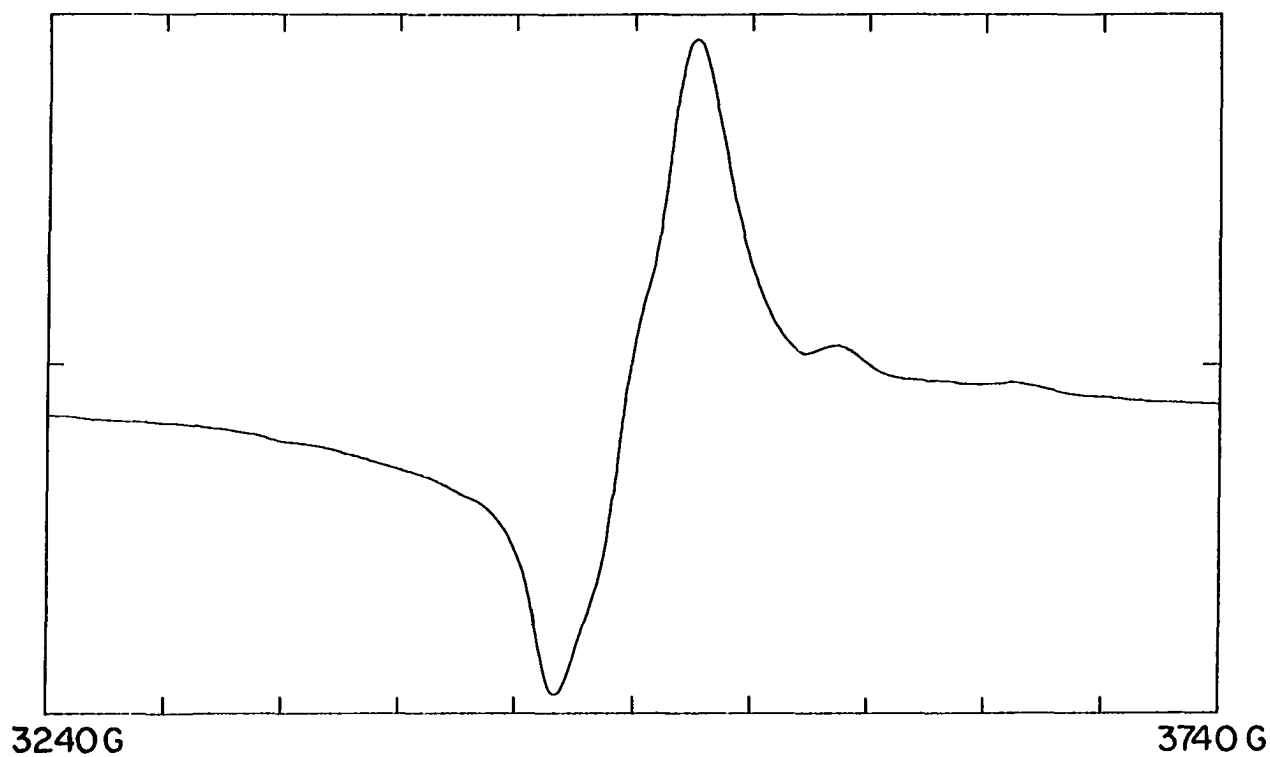

Figure 6. Room temperature electron spin resonance spectrum of $Mo_{1.0}Cl_{1.1}py_{0.8}$

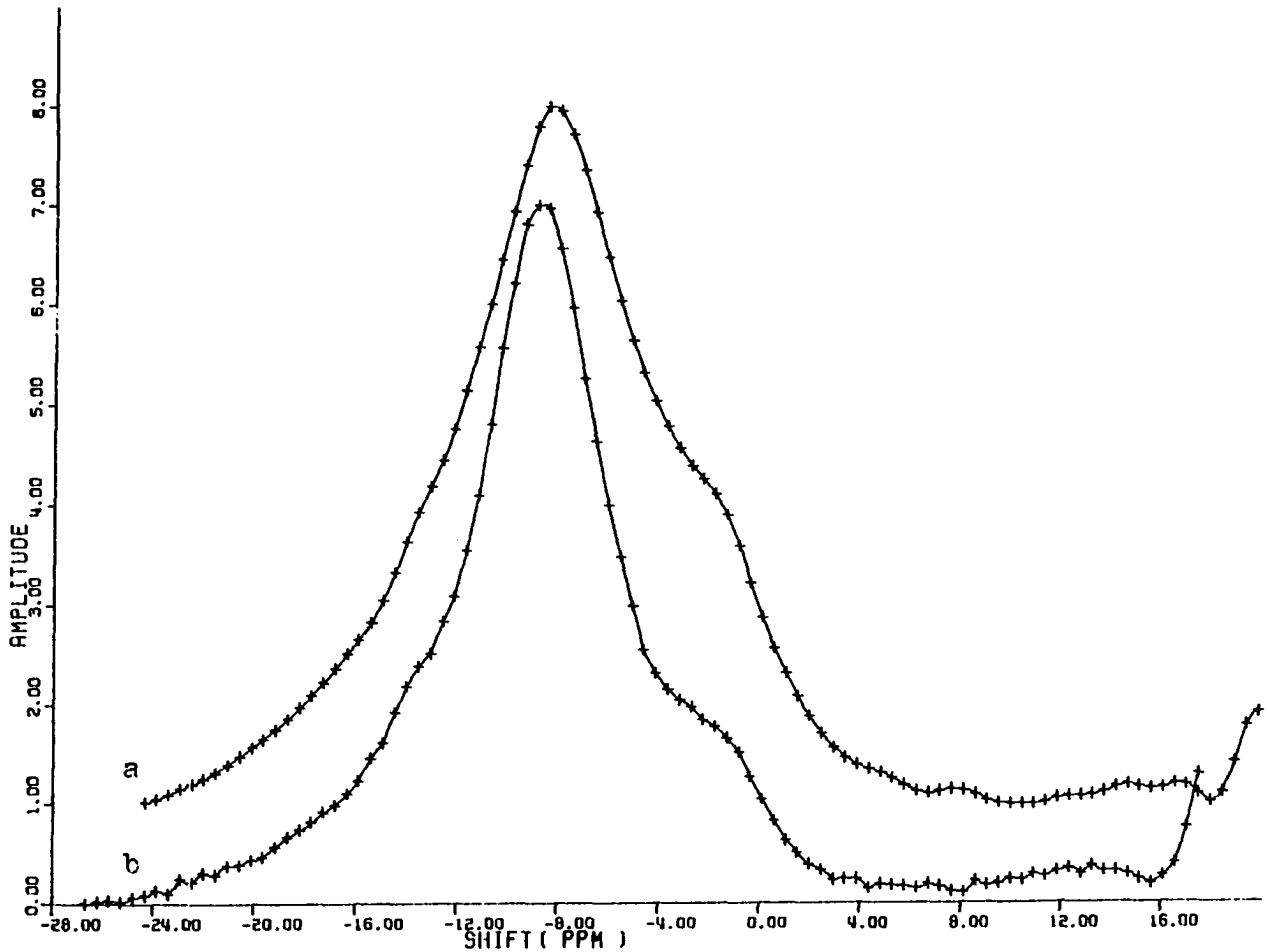

Figure 7. Combined rotation and multiple pulse proton nuclear magnetic resonance spectra of material washed in concentrated HCl(aq), a; material washed in concentrated DCl (in D_2O), b

washed material. Because deuterium should not appear in a proton spectrum, two possible explanations of the similarity of the two spectra are (1) no hydride is present and the asymmetric signal is due solely to the pyridine; (2) a hydride is present, but it does not originate from the hydrogen in the acid wash. The hydride, if present, must be formed prior to the acid wash. The limited resolution of the solid state NMR makes it impossible to confirm the existence of a hydride in this case.

X-ray photoelectron spectroscopy provides some interesting data capable of contributing structural insight. Figure 8 is a typical chlorine x-ray photoelectron spectrum. The spectrum can be satisfactorily accounted for by two types of non-equivalent chlorine atoms. The low binding energy doublet has been assigned to a terminal chlorine:[52] the 2p 3/2 peak is positioned at 198.5 eV with a FWHM of 1.22 eV. The high binding energy doublet has been assigned to the bridging chlorine atoms:[52] the 2p 3/2 peak is positioned at 199.4 eV with a FWHM of 1.22 eV. The 0.9 eV separation between the terminal and bridging chlorines is indicative of the doubly bridging chlorines found in molybdenum dimers, rather than the 2.3 eV separation between the terminal and triply bridging chlorines of $Mo_6Cl_{12}L_6$ compounds.[52] The spin-orbit splitting is 1.60 eV with a ratio of terminal chlorines to bridging chlorines of about 1.5:1.0. The com-

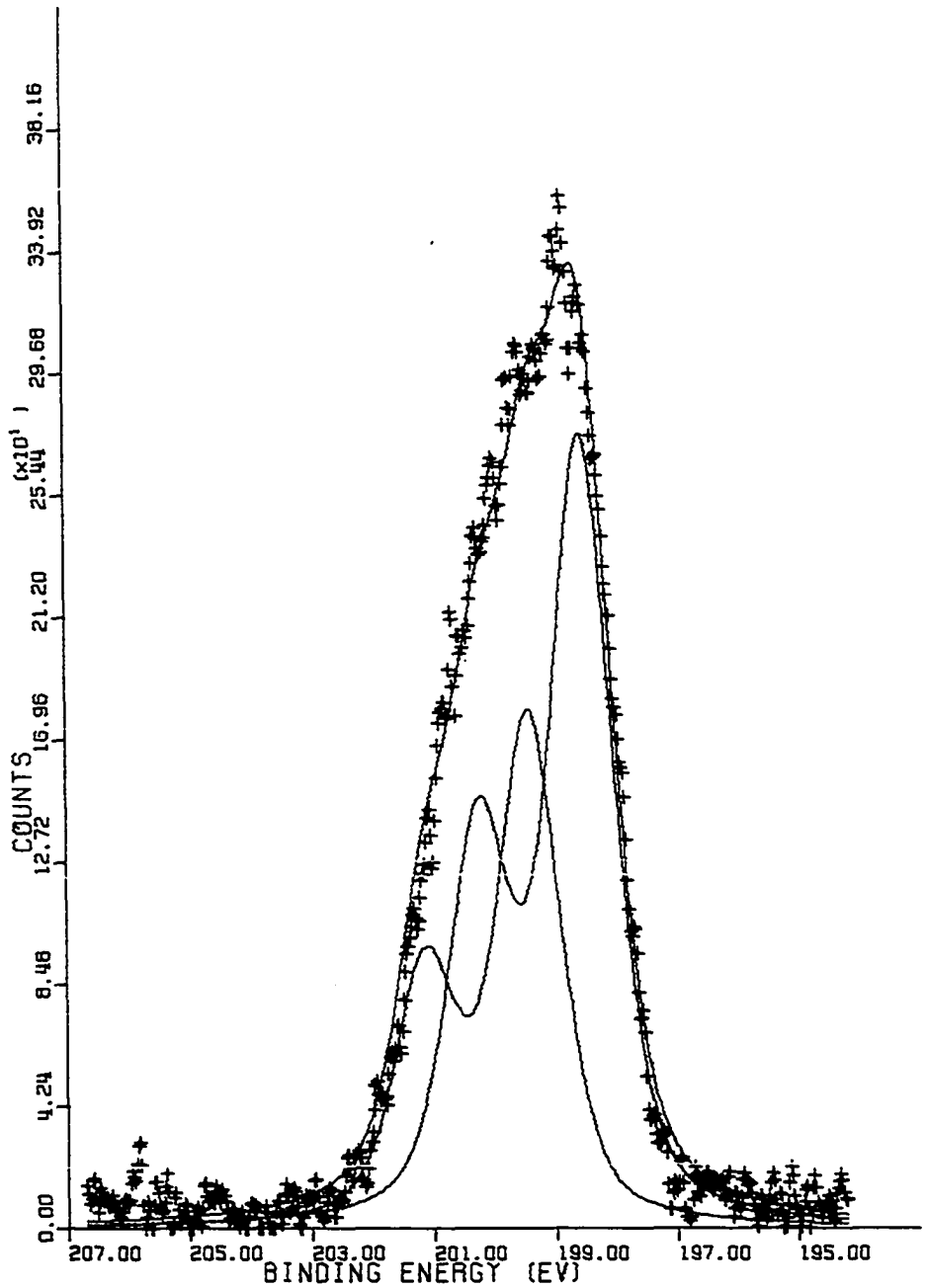

Figure 8. Chlorine 2p x-ray photoelectron spectrum of $Mo_{1.0}Cl_{1.1}py_{0.8}$

position can now be written $Mo_{1.0}(Cl_T)_{0.7}(Cl_B)_{0.4}py_{0.8}$.

Less likely assignments of these peaks are doubly bridging chlorine (198.5 eV) and triply bridging chlorine (199.4 eV). Doubly and triply bridging chlorine appear at 199.2 eV and 200.5 eV, respectively, in Mo_6Cl_{12}.[52] In the present study, the peaks may be shifted to lower binding energies if the chlorine environments are significantly different than in the Mo_6Cl_{12} cluster or if the molybdenum is in a substantially lower oxidation state.

The molybdenum x-ray photoelectron spectrum shows only one type of molybdenum, the 3d 5/2 peak appearing at 229.0 eV with a FWHM of 1.60 eV. The binding energy of this molybdenum species compares favorably with the 229 to 230 eV values routinely observed for Mo(II).[53] The assignment of oxidation state based on metal binding energies is sometimes a tenuous one. Within a related series of compounds the correlation of binding energy with oxidation state is fairly good, but care must be exercised in isolated studies. The presence of only one type of molybdenum discredits the existence of a mixture of molybdenum metal and a molybdenum compound. It also makes it unlikely that $Mo_{1.0}Cl_{1.1}py_{0.8}$ is a mixture of two or more distinct compounds: it would be improbable that all the components would give essentially identical molybdenum spectra unless they are very similar in structure.

Thin layer chromatography was unable to effect any separation of the material. This also suggests $Mo_{1.0}Cl_{1.1}py_{0.8}$ is not a mixture of different compounds.

$Mo_{1.0}Cl_{1.1}py_{0.8}$ is amazingly stable at elevated temperatures. Heating at 210° C overnight under a dynamic vacuum does not change the composition. The chemically determined oxidation state of 0.4+ is also not significantly changed (see Table I). The chlorine x-ray photoelectron spectrum of the heated material (Figure 9) is very similar to the unheated material (Figure 8). The heated material has a low binding energy 2p 3/2 peak at 198.3 eV with a FWHM of 1.22 eV, and a high binding energy 2p 3/2 peak at 199.2 eV with a FWHM of 1.22 eV. If these peaks are assigned to terminal and bridging chlorine, the ratio of terminal to bridging chlorines is 1.21:1.00. Any difference in the x-ray photoelectron spectrum of the heated material compared to the spectrum of the unheated material may be due to instrumental resolution. The ESR spectrum of this material (Figure 10) has a g of 1.95 and is much broader than the spectrum of the unheated material. The peak-to-peak separation is 133 G in the heated material compared to 59 G in the unheated material. The black powder obtained after heating remains amorphous.

Heating $Mo_{1.0}Cl_{1.1}py_{0.8}$ in a dynamic vacuum for 26 hours at 300°C causes only minimal change in the stoichi-

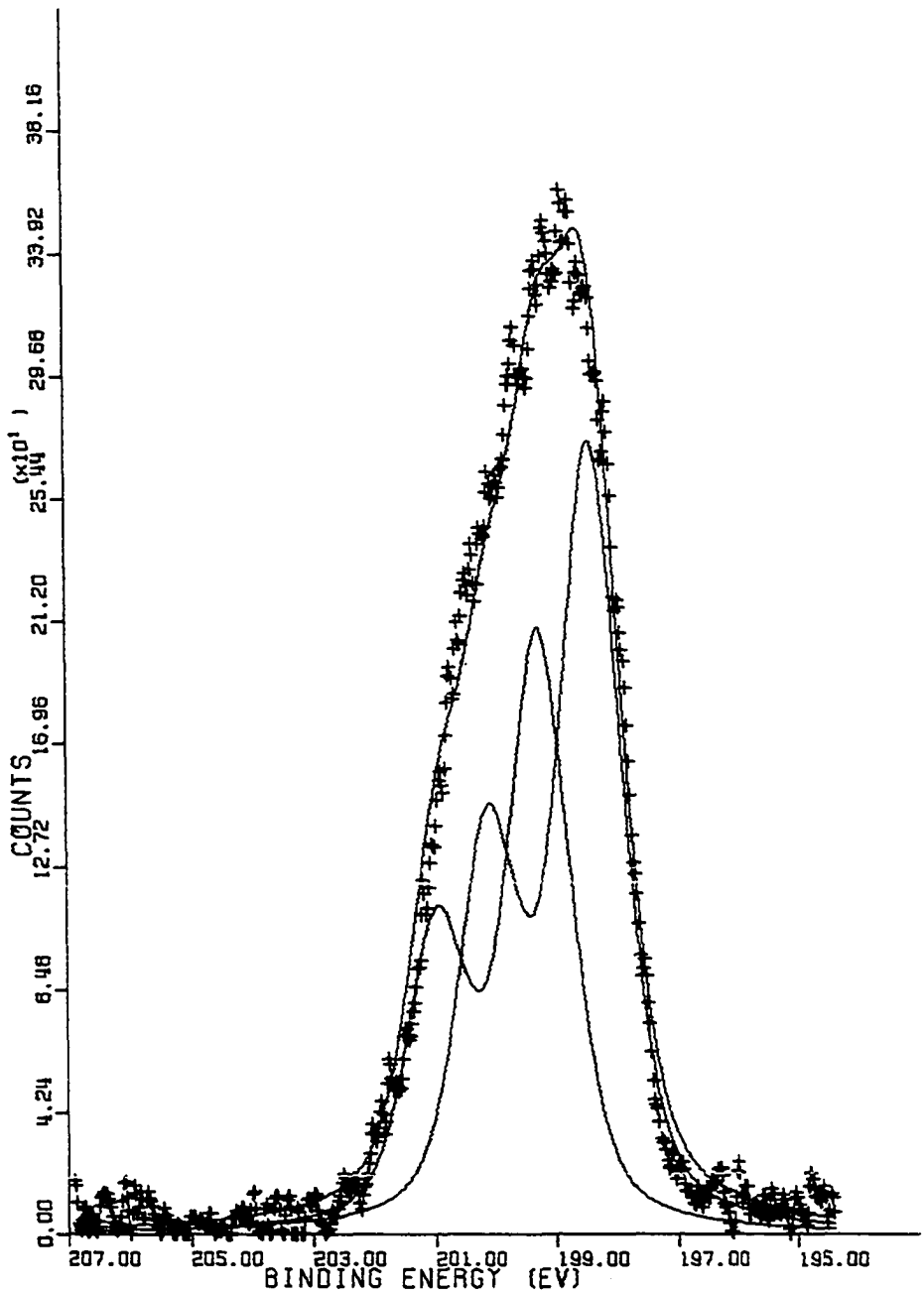

Figure 9. Chlorine 2p x-ray photoelectron spectrum of $Mo_{1.0}Cl_xpy_{0.8}$

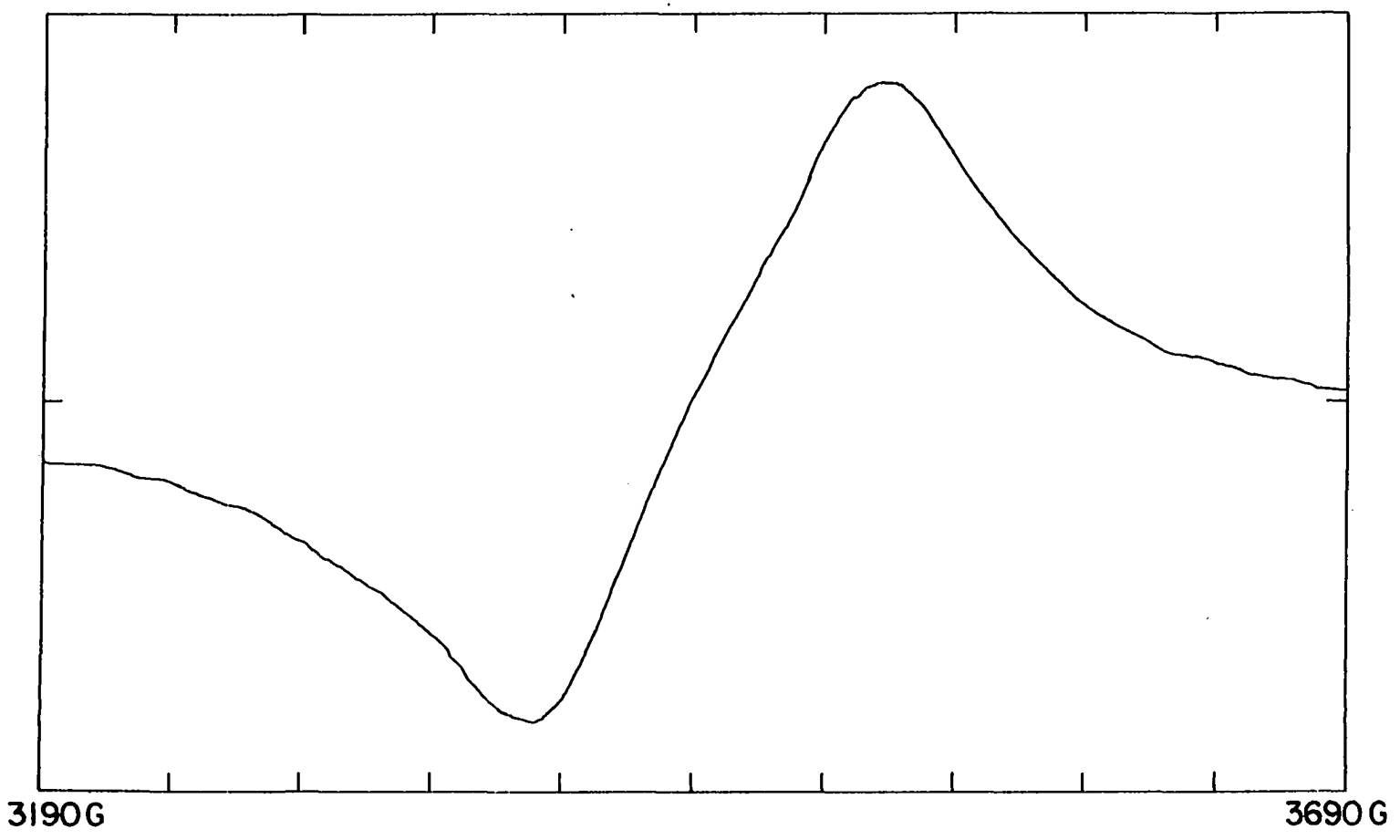

Figure 10. Room temperature electron spin resonance spectrum of $Mo_{1.0}Cl_xpy_{0.8}$

ometry: $Mo_{1.0}Cl_{1.0}py_{0.8}$. The infrared spectrum is listed in Table II. A small amount of a white-gray solid, probably pyH^+Cl^-, sublimed from the sample and a dark film or mirror formed. The evolved condensables, which were collected in a trap at -196°C, turned into a red liquid upon warming to room temperature and gave an infrared spectrum (1626s, 1595s, 1520s, 1473s, 1420w, 1363w, 1325m, 1236s, 1185m, 1152m, 1080w, 1051s, 1027m, 991s, 925w, 891m, 872m, 741s, 669s cm^{-1}) similar, but not identical to pyridine. On this particular sample the experimental oxidation state change upon heating, from 0.1+ to 0.0, is not considered significant. This sample was also amorphous.

Heating $Mo_{1.0}Cl_{1.1}py_{0.8}$ at 425°C for 63 hours in a dynamic vacuum caused decomposition. After heating, the reaction vessel was ringed with very narrow multi-colored bands. Analysis of the amorphous black-gray bulk residue showed it to be $Mo_{1.0}Cl_{0.7}C_{3.7}H_{1.7}N_{0.8}$. The pyridine thus was decomposed and no pyridine bands were observed in the infrared spectrum.

The thermal stability observed for $Mo_{1.0}Cl_{1.1}py_{0.8}$ lends limited support to the polymeric or extended view of the structure. It is generally assumed the crystalline form of a material is favored thermodynamically. Heating many amorphous materials permits them to crystallize, often at temperatures well below their melting points.[54] As $Mo_{1.0}$

$Cl_{1.1}py_{0.8}$ does not form a crystalline phase at higher temperatures, and decomposes instead of melting, the argument in favor of an extended structure instead of a well-formed disordered cluster can be made.

Attempts to synthesize a crystalline derivative of $Mo_{1.0}Cl_{1.1}py_{0.8}$ were not successful. The reaction with iodine in refluxing acetonitrile produces an intractable tar. Refluxing $Mo_{1.0}Cl_{1.1}py_{0.8}$ in acetic acid resulted in the coordination of acetate. The product, $Mo_{1.0}Cl_{0.7}(C_5H_5N)_{0.7}(C_2H_3O_2)_{0.5}$, shows coordinated pyridine and acetate in the infrared spectrum, and the x-ray powder pattern shows it is amorphous.

CONCLUSIONS

Despite extensive study, $Mo_{1.0}Cl_{1.1}py_{0.8}$ remains an enigma. The techniques employed, singly and collectively, give no unambiguous description of the structure; furthermore, some of the data are conflicting. Enough has been learned to permit limited statements and some speculation about what $Mo_{1.0}Cl_{1.1}py_{0.8}$ is and is not. Formulating $Mo_{1.0}Cl_{1.1}py_{0.8}$ as a mixture of molybdenum metal and a molybdenum, chlorine, pyridine compound has the attraction of explaining the low apparent oxidation state and low coordination number. This is not the proper explanation as is demonstrated by its complete solubility in pyridine, its completely amorphous nature and the presence of only one type of molybdenum in the x-ray photoelectron spectrum. The same argument, with less conviction, can be applied to the coexistence of two or more distinct compounds. It seems unlikely, but not impossible, that the morphology of the particles, the solubilities, and the molybdenum x-ray photoelectron spectra would be so similar as to not even hint at this coexistence. It should be noted that the FWHM of the molybdenum peak in the x-ray photoelectron spectrum is rather broad (1.6 eV) and this could be the result of several types of molybdenum atoms in quite similar environments. The mixture of two or more discrete compounds does not even explain the low experimental oxidation state.

A highly bridged metal-metal bonded cluster or polymer model of $Mo_{1.0}Cl_{1.1}py_{0.8}$ seems to be the only plausible explanation of the low ligand to metal ratio. Yet it is not easy to propose a possible structure for such a material. There are severe constraints: the x-ray photoelectron spectrum indicates the molybdenum atoms are identical, or at least very similar, and the ratio of terminal to bridging chlorine atoms dictates an average of 0.7 terminal and 0.4 bridging chlorine atoms per molybdenum. The pyridine may not even participate in bridging. There seems to be no precedent for the nitrogen of a pyridine bridging two metals. The abstraction of a hydrogen atom from pyridine with subsequent formation of a molybdenum-carbon bond also seems unreasonable; the H:C ratio is not consistently low and such a bond should induce drastic changes in the pyridine infrared spectrum, which are not observed.

The introduction of hydrides into the above model increases the ligand to metal ratio but still does not account for the chemically determined oxidation state. There is no definitive evidence of any hydride ligand and great caution must be exercised in considering hydride ligands as the solution to the oxidation state antinomy.

An interesting explanation of the low molybdenum oxidation state is the formation of a protonic species. Many neutral organometallic compounds can be protonated at the

metal to form $(MH)^+$ species: $(C_5H_5)_2H_2Re^+$, $(C_5H_5)_2H_3Mo^+$, $HOs_3(CO)_{12}^+$, and $HNi(P(OC_2H_5)_3)_4^+$ are examples.[3] If such a species were formed in the present work, the proton would be subject to detection by the techniques discussed for a metal hydride, but the oxidation state of the molybdenum would be very low. If a protonated species is formed, the acid wash of the black material might be described by $Mo_{1.0}Cl_{0.6}py_{1.2} + \frac{1}{2}HCl \longrightarrow H_{0.5}Mo_{1.0}Cl_{1.1}py_{0.8}$ where the molybdenum has an oxidation state of 0.6+. This model provides a means for including hydrogen in the formula and resolving the conflict between oxidation state and electrical neutrality. The model does not provide additional information about the structure of $Mo_{1.0}Cl_{1.1}py_{0.8}$.

Finally, the amorphousness of $Mo_{1.0}Cl_{1.1}py_{0.8}$ does not permit an exact solution of the structure but is consistent with a polymer or extended structure. However, it does not exclude other descriptions of the material.

PART II. MIXED SULFUR CHLORINE SUBSTITUTED HEXANUCLEAR MOLYBDENUM CLUSTERS

INTRODUCTION

Superconductivity, the loss of electrical resistance in many metals and compounds at very low temperatures, was discovered by Kamerlingh Onnes in 1911. He noted that mercury abruptly lost all electrical resistance slightly below 4.2°K and later found transition temperatures of 7.2°K for lead and 3.7°K for tin. The practical applications of this discovery were not lost on him, and in 1913 he attempted to construct a superconducting magnet from a coil of lead.[55] Such a superconducting magnet should produce a very powerful magnetic field without generating heat or wasting energy. It might also produce a magnet capable of generating fields larger than the two tesla limit imposed on conventional magnets by the saturation limit of iron. The lead magnet was superconducting only when the current was small. It reverted to the resistive state when the magnetic field reached a strength of a few hundred gauss, even at temperatures well below the critical temperature (T_c) of lead.[56] All pure-metal superconductors undergo this sudden quenching of superconductivity at a well-defined critical field (H_c) on the order of 1000 gauss.[55]

In the 1920s, magnetic alloys were discovered which retained vestiges of superconductivity at much higher magnetic fields. For example, de Haas and Voogd found that

lead-bismuth alloys transformed to the normal state over a range of fields up to 20,000 gauss.[57,58]

Superconductors are now classified as Type I or Type II.[59] Type I superconductors undergo a sharp superconductor-normal conductor transition at low temperatures and have low values of H_c. Type II superconductors behave like Type I materials when in the presence of very weak magnetic fields. At some critical field, H_{c1}, Type II materials become a mixture of superconducting and normal material, and the last trace of superconductivity does not vanish until a much larger field, H_{c2}, is applied.

The discovery that A15 compounds were Type II superconductors with high critical fields made superconducting magnets a possibility.[60] The technological problems of constructing such magnets are being overcome, and today most superconducting magnets are constructed of either Nb-Ti alloys or the A15 compound Nb_3Sn. $Nb_{38}Ti_{62}$ magnets have an upper limit of about 8 teslas while a mixed Nb_3Sn-V_3Ga magnet has been operated at 17.5 teslas.[55] The Nb_3Sn-V_3Ga magnet represents the maximum field yet attained, and most superconducting magnets operate in the range of 3 to 8 teslas. It is therefore understandable that the discovery of a critical field of 60 teslas in the compound $PbMo_6S_8$[61,62] generated much excitement.

A material's superconductivity is quenched not only

when the temperature exceeds T_c or the applied field exceeds H_c, but also if the current it carries surpasses the critical current density (J_c). Wires of $PbMo_6S_8$ have J_c of about $2x10^7$ A/m^2 at 4.2°K and 4 T.[63,64] These wires were fabricated by reacting molybdenum wire or tape in an atmosphere of sulfur and then lead for several hours between 800° and 1100°C. Wires fabricated from bulk $PbMo_6S_8$ have current densities on the order of $5x10^7$ A/m^2 at 4.2°K and 4 T.[65] Films of $PbMo_6S_8$ have J_c values of about $5x10^7$ A/m^2 in an applied field of 15 T at 1.8°K.[66] These critical currents are all several hundred times less than for Nb_3Sn. In addition, $PbMo_6S_8$ and related compounds are very brittle. Despite these disadvantages, $PbMo_6S_8$ can not be ignored as a candidate for high field superconducting magnets.

$PbMo_6S_8$ is a member of a series of ternary molybdenum chalcogenides discovered by Chevrel in 1971. Actually, the first reported member was described as "$SnMo_6S_7$" by Espelund in 1967,[67] but it was Chevrel and co-workers who realized a whole class of related compounds existed. The binary analogues Mo_6Se_8 and Mo_6Te_8 had also been reported several years earlier.[68] These compounds, often called the Chevrel phases, have the formula $M_xMo_6X_8$ where M is a metal cation and X is S, Se, or Te. The initial paper by Chevrel and co-workers[69] reported compounds with M = Ag, Sn, Ca, Sr, Pb, Ba, Ni, Co, Fe, Mn, Cr, Cu, Mg, Zn, Cd, Li, Na, K, Rb, and Cs. It is

now known that M can also be Al, Ga, Y, Nb, Pd, In, Hg, Tl, the lanthanide series (except Pm), Th, and U as well as mixed metal phases like $Pb_{1-x}Eu_xMo_6S_8$. These ternary phases can be divided into two classes: those containing "large" ternary metals like Pb or Sn and those containing "small" ternary metals like Cu or Co.[10,11]

The group of compounds containing large metals tends to be stoichiometric with x very close to 1. Most of these crystallize in the rhombohedral space group $R\bar{3}$ and have α between 88° and 90°. As a group, the large cation materials tend to have high critical temperatures, usually between 6° and 15°K. Conversely, the "small" cation materials form solid solutions over a range of x values. The copper compound $Cu_xMo_6X_8$ is typical of this second class and values of x between 1.5 and 4 are known. The "small" cation materials are usually rhombodedral $R\bar{3}$, have α between 93° and 96°, and have lower critical temperatures than the "large" cation compounds.

In addition to the binary compounds Mo_6S_8,[70] Mo_6Se_8,[68] and Mo_6Te_8,[68] numerous pseudobinary compounds of the type $M'_yMo_{6-y}X_8$ exist. Examples of these mixed metal compounds are $Re_4Mo_2S_8$, $Ru_2Mo_4Se_8$, $Nb_{0.75}Mo_{5.25}Se_8$ and $Rh_{1.33}Mo_{4.66}Te_8$.[71] Another class of pseudobinary compounds has the formula $Mo_6X_nY_{8-n}$ and include compounds such as $Mo_6S_6O_2$,[72] $Mo_6S_6Br_2$,[73] $Mo_6Se_5Cl_3$,[71] and $Mo_6Te_6Cl_2$.[71] Still other analogues

are known: $Ru_2Mo_4Se_{8-n}Te_n$,[71] $M_xMo_6S_6O_2$,[72] and $PbMo_6S_{8-n}Se_n$.[74]

The structure of the Chevrel phases and all related compounds is based on the Mo_6X_8 cluster[10,11] which is shown in Figure 11. The structure can be described as a cube of X atoms with a Mo atom centered on each face. These Mo atoms form an octahedron, and an alternate view of the Mo_6X_8 unit is that of a metal octahedron having each face capped with a triply bridging X atom. The unique structure of the Chevrel phase is a result of the linkage of the Mo_6X_8 units in the lattice. Each molybdenum atom has a terminal ligand which is shown in Figure 12. This is possible because the Mo_6X_8 units are arranged in a rhombohedral lattice (Z = 1). Each unit is rotated by approximately 26° about the ternary axis from the position where all the X cubes are aligned. The Mo_6X_8 unit is slightly elongated along the ternary axis of the rhombohedral cell creating pseudocubes of X atoms, and the molybdenum atoms are displaced approximately 0.25Å above the faces of this pseudocube. In Mo_6S_8[70], there are two different intracluster Mo-Mo distances: 2.698Å and 2.862Å. In addition the closest intercluster Mo-Mo distance is 3.084Å.[70] The two shortest S-S distances within a cluster are 3.310Å and 3.550Å. The average Mo-S intracluster distance is 2.44Å while the shortest Mo-S intercluster distance is 2.425Å.

If "large" M atoms are present, they are located at the

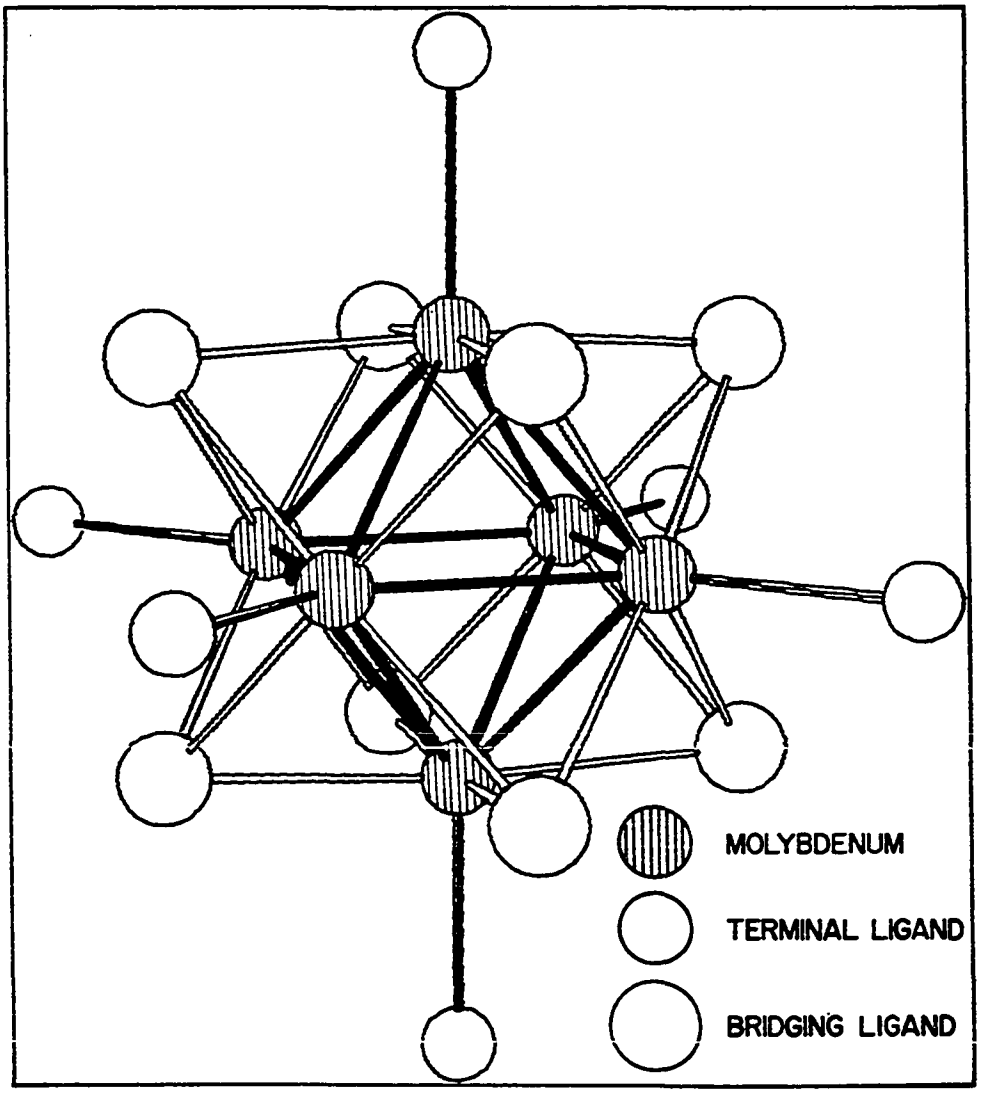

Figure 11. Structure of Mo_6X_8 cluster

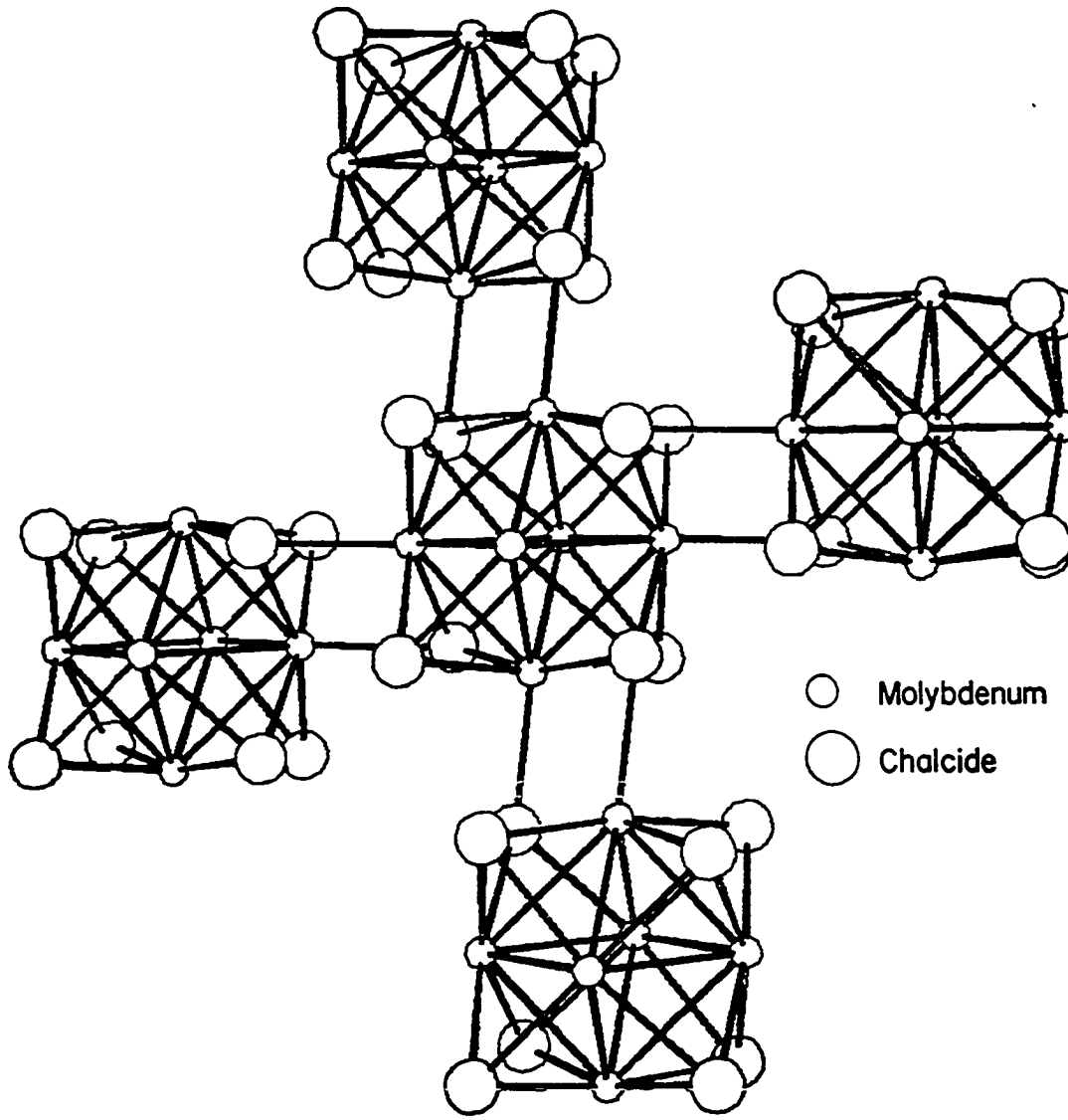

Figure 12. Arrangement of Mo_6X_8 clusters in the Chevrel phases (two of the six neighboring clusters have been deleted for clarity)

origin of the rhombohedral cell.[10,11] This position is surrounded by a pseudocube of sulfur atoms, the distortion being a slight compression along the ternary axis. The "small" cation case is more complicated.[10,11] In these compounds, the "small" cations have very large thermal parameters perpendicular to the ternary axis. The large thermal parameters are believed due to delocalization of the M atoms from the center of the X pseudocube. It is thought that the M atoms move toward the six non-unique corners of the sulfur pseudocube. In the case of $Cu_{2.76}Mo_6S_8$ these positions, which form a nearly planar hexagon with $\bar{3}$ symmetry, are separated from their immediate neighbors by 1.306Å.[75] In addition to these six "inner" positions, there are six "outer" sites located about half way along the rhombohedral axes. An "inner" position and its closest "outer" neighbor are separated by about 1.330Å in $Cu_{2.76}Mo_6S_8$. In this compound, the "inner" positions are 24% occupied and the outer positions are 22% occupied. The proximity of adjacent "inner" sites, as well as neighboring "inner" and "outer" sites, prohibits their simultaneous occupancy and places an upper geometrical limit of six "small" M atoms per Mo_6S_8 unit.

Some of the "small" cation compounds undergo a disorder-order transition from rhombohedral to triclinic symmetry. Concomitant with the change of symmetry is an ordering of the M atoms; they form pairs and are centered on the corners

of the triclinic cell. The M-M distance in the triclinic form of $Cu_{1.80}Mo_6S_8$[76] is 2.58Å and in $Fe_2Mo_6S_8$[77] the M-M distance is 2.513Å.

Several molecular-orbital and band calculations have been performed on the Mo_6X_8 and $M_xMo_6X_8$ clusters.[78-83] These calculations differ in the details but agree sufficiently to permit a qualitative understanding of the Chevrel phases. Covalent mixing of the sulfur 3s and 3p orbitals and the molybdenum 5s orbitals produces a filled valence band and an empty conduction band. Sulfur, therefore, has a valency of 2- as indicated by the sulfur-sulfur distances. Above these primarily sulfur bands are the molybdenum 4d bands: 12 of the 30 molybdenum states are separated from 18 higher lying d states by a forbidden energy gap of 1 to 2 eV. The lower 12 molybdenum d states can hold 24 electrons and are grouped into five narrow sub-bands: T_{1u}, T_{2g}, A_{1g}, T_{2u}, and E_g. The ordering of these bands is not certain. Some workers believe the E_g band is the highest lying of the five,[82] while others believe the T_{2u} is the highest.[80] The Fermi level (E_f) lies near the top of this complex and is primarily of $d_{x^2-y^2}$ character. Weak intercluster coupling of the $d_{x^2-y^2}$ orbitals results in narrow bands at E_f and a high density of states.

The five bonding Mo d bands can accommodate 24 cluster electrons, so named because the orbitals arise predominantly

from the cluster of six atoms comprising the molybdenum octahedron. Mo_6X_8 has 20 cluster electrons, leaving these bands only partially filled. Depending upon the exact ordering of bands near E_f, these compounds should be either semiconductors or metals. The ternary metal atoms in the Chevrel phases appear to function principally as donors of electrons to the Mo_6 cluster. The series $Cu_xMo_6S_8$,[75] x = 1.80, 2.76, 2.94 and 3.66 should have 21.80, 22.76, 22.94 and 23.66 electrons respectively in the molybdenum 4d bonding bands. Accompanying the increase of cluster electrons is a decrease of the average intracluster molybdenum-molybdenum distance: 2.718Å, 2.690Å, 2.681Å, and 2.670Å, respectively. The contraction of the Mo_6 cluster is consistent with the filling of bands localized between intracluster molybdenum atoms and the donation of electrons from the copper atoms. The copper atoms appear to exist as monovalent cations and the x = 3.66 compound approaches the electronically imposed phase limit of 24 cluster electrons for $Cu_4Mo_6X_8$.

The upper limit of 24 cluster electrons is persistent throughout the Chevrel phases. $Y_{1.2}Mo_6S_8$, $In_{1.2}Mo_6S_8$, $Co_2Mo_6S_8$ and $Mo_2Re_4S_8$ are all representative of compounds with the limit of approximately 24 cluster electrons. There are a few compounds whose stoichiometry suggest more than 24 cluster electrons: $Al_3Mo_6S_8$, $Ga_2Mo_6S_8$ and $NbMo_6S_8$ are exam-

ples. Instead of the 29, 26 and 25 cluster electrons suggested by the formulas, it is believed that the cluster bands only accept 24 electrons and the superfluous electrons reside on the ternary metal.[84] Compounds with 24 cluster electrons are generally insulators or semiconductors, while those with between 20 and 24 cluster electrons tend to be metallic at room temperature and superconducting at low temperatures. These properties are generally consistent with the filling of the conduction band as predicted by the band calculations.

The structure of the molybdenum dihalides, like the Chevrel phases, is based on the Mo_6X_8 motif. They differ only in the manner the Mo_6X_8 units are connected. The two axial terminal ligands in the dihalides are not shared with adjacent clusters and the equatorial terminal ligands are shared equally between two clusters. The dihalides can be written $(Mo_6X_8)X_{4/2}X_{2/1}$ where the 4/2 signifies four halides shared equally between two clusters and the 2/1 corresponds to the two axial halides which are not shared. This formula obviously reduces to Mo_6X_{12} which is the accurate formula of the molybdenum dihalides.

The structural similarity of the Chevrel phases and the molybdenum dihalides imposes analogous electronic structures. The Mo_6 clusters in the dihalides also have 12 bonding and 18 antibonding molybdenum 4d orbitals.[78] The 12 bonding orbitals

are completely filled by the 24 cluster electrons and the compounds are insulators.

The structural resemblance of the molybdenum dihalides and the Chevrel phases suggests it should be possible to interconvert them with appropriate chemical reactions. The binary and ternary Chevrel phases are usually made by mixing stoichiometric amounts of the elements or compounds of the elements (like Mo_2S_3 and M_xS) in an evacuated, sealed quartz tube and heating between 900° and 1200°C from one to seven days. Typically the resulting material is ground up and heated several times to ensure a uniform product.[69] It is not possible to synthesize Mo_6S_8 by this method because it is unstable above 468°C.[70] Mo_6S_8 can be made by leaching the ternary metal from $NiMo_6S_8$ or $CuMo_6S_8$ with hydrochloric acid. Mo_6Se_8 and Mo_6Te_8 do not suffer this thermal instability and can be prepared by the direct method. Mixed metal, mixed chalcogen and chalcogen-halide products can often be prepared by the direct method if the appropriate starting materials are employed.

The above high temperature method sometimes fails to produce the desired Chevrel phase. One method of preparing recalcitrant compounds involves heating the ternary metal with Mo_6S_8 below 468°C. Compounds containing Al, Ga, Tl, Nb, and Hg have been prepared by this method.[70,84] Another circuitous process of preparing the Chevrel phases is the ca-

thodic insertion of the ternary metal into Mo_6S_8 at room temperature utilizing electrolysis of aqueous and non-aqueous solutions of ternary metal salts.[85]

At some point these three methods of preparation all involve a minimum temperature of 1000° C, since Mo_6S_8 must first be prepared from $M_xMo_6S_8$. A lower temperature synthesis of the Chevrel phases would not only be convenient, but might make possible the direct synthesis of Mo_6S_8 and related compounds which are unstable at high temperatures. The systematic substitution of halides in the molybdenum dihalides by chalcogenides might provide such a low temperature route. A review of the chemistry of molybdenum dihalides shows that the cluster may be amenable to substitution by sulfur resulting in Mo_6S_8 type products.

The $Mo_6Cl_8^{4+}$ cluster is very robust as evidenced by its inertness to boiling aqua regia, concentrated sulfuric acid heated to fuming, and nitric acid, although it can be decomposed by aqueous alkali.[86] The outer ligands of $(Mo_6X_8)X_4$ (X = Cl, Br, I) can be readily substituted. Derivatives such as $(Mo_6X_8)X_4L_2$ where L is H_2O,[87] py,[87] DMF,[88] DMSO,[88] NMe_3,[89] NEt_3,[89] γ-pic,[89] quinoline,[89] pyrazine,[89] pyO,[90] and PPh_3[90] are common and can usually be produced with only slight warming. Recrystallization of $(Mo_6Cl_8)Cl_4$ from HBr or HI followed by drying yields $(Mo_6Cl_8)Br_4$ or $(Mo_6Cl_8)I_4$.[87] $(Mo_6Cl_8)(OH)_4 \cdot 14H_2O$ has been prepared by precipitating dissolved

Mo_6Cl_{12} with aqueous ammonia-ammonium nitrate buffer.[87] Other compounds which have resulted from complete removal of the outer halides are of the type $((Mo_6Cl_8)L_6)(ClO_4)_4$, L = DMF,[88] DMSO;[88] $Na_2((Mo_6Cl_8)(OR)_6)$, R = CH_3,[91] C_2H_5,[91] C_6H_5;[92] and various salts of $((Mo_6Cl_8)L_6)^{2-}$, L = (NCS^-),[93,94] (SCN^-),[93,94] (N_3^-),[93,94] (NCO^-),[93] $(NCSe^-)$,[93,94] (CH_3S^-),[94] $(C_6H_5CH_2S^-)$.[94]

Substitution of inner halides is more difficult. Halide exchange in melts gives complete replacement as in Mo_6Cl_{12} + excess LiX $\xrightarrow{\text{melt}}$ Mo_6X_{12} (X = Br, I).[95] Mixed halide compounds of the type $(Mo_6X_8)X'_4$ can be thermally converted to $(Mo_6X_4X'_4)X_4$ where X' is a heavier halide than X.[96] The reaction of HgY_2 and $(Mo_6X_8)X_4$ results in the opposite direction of substitution:[97]

$$(Mo_6Br_8)Br_4 \xrightarrow{HgCl_2} Hg(Mo_6Cl_8)Cl_6$$
$$\xrightarrow{HgBr_2} Hg(Mo_6Br_8)Br_6$$
$$\xrightarrow{HgI_2} Hg(Mo_6Br_8)I_6.$$

Replacement of inner halides by non-halide ligands have also been reported. Alkoxide substitutions have produced $Na_2((Mo_6(OCH_3)_8)(OCH_3)_6)$,[91] $Na_2((Mo_6(OCH_3)_8)(OC_6H_5)_6)$,[92] and $Na_2((Mo_6(OCH_3)_4(OC_6H_5)_4)(OC_6H_5)_6)$.[92] Recently there has been a report of $((Mo_6Cl_7S)Cl_6)^{3+}$ and $(Mo_6S_6Cl_2)(NC_5H_5)_6$ having been prepared.[98] Although these last two compounds consist of isolated clusters, the retention of the Mo_6X_8 unit demonstrates the feasibility of inserting sulfur into the

inner ligand positions of the Mo_6Cl_{12} cluster and producing analogues of the Chevrel phases.

The thesis of this research is the synthesis of Mo_6S_8 or $(Mo_6S_8)L_6$ by substituting sulfur for chlorine in Mo_6Cl_{12}. The existence of such a low temperature preparation of Mo_6S_8 would not only offer a convenient route to the Chevrel phases, but would provide excellent opportunities to investigate the chemistry of systematically substituted molybdenum dihalides, as with members of the series $(Mo_6S_{8-x}Cl_x)L_6$, $(x = 0, 1, \ldots, 7)$. Such a series would permit the systematic study of the Mo_6X_8 cluster's electronic structure.

EXPERIMENTAL METHODS

Most chemicals were reagent grade and generally were used without further purification. They were stored in a dry box, when necessary, until needed. Commercial $AlCl_3$ required purification by sublimation before use. Mo_6Cl_{12} and NaSH were prepared as previously reported.[99,100] Na_2S was prepared by the addition of sulfur to a stoichiometric amount of sodium in liquid ammonia. This addition was carried out in a specially designed reaction vessel. Clean sodium was placed in the reaction vessel and dry ammonia was distilled into the vessel. Following dissolution of the sodium, a pre-weighed amount of sulfur was slowly added from a side arm while maintaining the vessel temperature at approximately -75°C. After the sulfur addition was complete the ammonia was permitted to boil off slowly. The product was then pumped dry under high vacuum. Care must be exercised to protect reactants and products from air. The Na_2S so prepared showed no significant impurities in either the infrared or x-ray photoelectron spectra. Calculated for Na_2S: S, 41.08%. Found: S, 41.05%.

Solvents required purification. ACS grade pyridine was dried by refluxing over phosphorous pentoxide or by standing over phosphorous pentoxide for two weeks. The pyridine was subsequently outgassed, vacuum distilled onto molecular

sieves, and vacuum distilled as required. 95% 3,5-lutidine was refluxed over phosphorous pentoxide, distilled under nitrogen and syringed under nitrogen as needed. ACS grade methanol was fractionally distilled, outgassed, vacuum distilled onto 3A molecular sieves and vacuum distilled as needed.

Most of the starting materials utilized were air sensitive and some products were pyrophoric. When appropriate, manipulations were performed under a blanket of purified nitrogen. Solvents were vacuum distilled when possible on a vacuum line with a working vacuum of 10^{-4} to 10^{-5} torr. Reaction vessels were loaded and emptied in a dry box containing an atmosphere of nitrogen. Samples for spectroscopic analysis were also prepared in a drybox. The atmosphere in the drybox was circulated over Chemalog catalyst R3-11 and molecular sieves to remove oxygen and water. The drybox atmosphere was periodically monitored by burning a 25 watt incandescent light bulb with the filament exposed to the atmosphere.

X-ray photoelectron spectra were accumulated with an AEI Model ES200B spectrometer. Samples were mounted on either adhesive tape or Ag-Cd alloy, and introduced directly from a helium-filled dry box into the instrument. Standard gun Al K_{α} radiation (K.E. = 1486.6 eV) was employed and spectra were referenced to the carbon 1s peak which was as-

signed a binding energy of 285.0 eV. Fifty to 100 scans were sufficient to obtain good quality molybdenum 3d spectra, while 200 to 300 scans were required for the 2p spectra of chlorine and sulfur. Spectra were deconvoluted into component bands with the APES computer program[46] (see Appendix).

Infrared spectra were obtained from 4000 cm^{-1} to 200 cm^{-1} as nujol mulls between CsI plates on a Beckman IR 4250 spectrometer or between 650 cm^{-1} to 50 cm^{-1} as nujol mulls between polyethylene sheets on an IBM Series 90 spectrometer. Electron spin resonance (ESR) spectra were recorded on a Varian E3 spectrometer. X-ray powder patterns were collected using a Debye-Scherrer camera (radius = 114.6 mm) and copper radiation. The x-ray powder pattern of $(Mo_6X_8)(C_5H_5N)_6$ (X = S, Cl) was calculated using a computer program[101] and structural data for $(Mo_6S_6Cl_2)(C_5H_5N)_6$.[98] In the single crystal x-ray structure determination, $(Mo_6S_6Cl_2)(C_5H_5N)_6$ was refined as $(Mo_6S_8)(C_5H_5N)_6$ because it was not possible to distinguish between the chlorine and sulfur atoms. In calculating the x-ray powder pattern, all X atoms were assumed to be sulfur atoms. The fifty most intense lines in the powder pattern from 8.29° to 42.27° in 2θ are listed in Table III.

Sodium, carbon, hydrogen and nitrogen elemental analyses were performed by the Ames Laboratory Analytical Services. Sulfur, as well as some carbon, hydrogen and nitrogen analyses were performed by Schwarzkopf Microanalytical Labo-

Table III. Powder x-ray diffraction data

A[a]	B[b]	C[c]	D[d]	E[e]
10.6617(100.0)	10.586(vs)	10.727(vs)	11.090(vs)	12.590(w)
9.2107(57.9)				11.539(w)
9.1425(43.6)	8.995(s,b)	9.229(s,b)	9.215(m)	10.406(s)
8.7681(45.4)				8.882(s)
7.9234(30.2)	7.932(s)	7.922(s)	8.253(s)	
7.3433(11.0)			7.625(m)	7.531(w)

[a]The fifty most intense lines from 8.29° to 42.27° in 2θ calculated for $(Mo_6X_8)L_6$. The intensities are given in parentheses.

[b]$(Mo_{6.0}S_{6.5}Cl_{1.4})Cl_{0.2}py_{2.8}$ is the product of 1 Mo_6Cl_{12} and 16 NaSH in refluxing pyridine for 6.7 days. The pattern matches that calculated for $(Mo_6X_8)L_6$. The estimated intensities are given in parentheses: very, v; strong, s; medium, m; weak, w; broad, b.

[c]$(Mo_{6.0}S_{5.3}Cl_{1.9})Cl_{0.5}py_{2.3}$ is the product of 1 Mo_6Cl_{12}, 4 NaSH and 4 Na_2S in refluxing pyridine for 7.0 days. The pattern matches that calculated for $(Mo_6X_8)L_6$.

[d]$Mo_{1.0}S_{2.3}py_{0.2}$ is the product of 1 Mo_6Cl_{12} and 16 NaSH in 225°C pyridine for 7.8 days. The pattern does not match that calculated for $(Mo_6X_8)L_6$.

[e]$(Mo_{6.0}S_{6.0}Cl_{3.5})Cl_{0.7}Lut_{5.0}$ is the product of 1 Mo_6Cl_{12} and 8 NaSH in refluxing 3,5-lutidine for 8.0 days.

Table III. (continued)

A	B	C	D	E
7.2525(16.6)	7.248(s)	7.278(s)		6.770(m)
6.3164(6.2)	6.338(m)	6.343(m)	6.219(s)	6.186(w)
5.8515(6.3)				
5.7992(2.0)			5.794(m)	5.688(s)
5.7317(14.7)	5.703(s)	5.747(s)		
5.7187(3.9)				
5.4221(11.3)				
5.3308(1.1)	5.246(m)	5.391(m)		
5.2067(1.1)				5.246(m)
5.0195(2.4)				
4.6054(1.8)	4.578(w)	4.600(w)		
4.2911(1.9)				
3.6964(1.1)				3.848(w)
3.6262(1.4)	3.627(w,b)	3.618(w,b)		
3.5814(1.5)				
3.5046(1.0)				
3.4044(1.0)				
3.1326(1.0)				3.236(w)
2.9975(1.8)				
2.9517(1.6)				
2.9104(1.4)				
2.7786(1.0)				2.746(w)

Table III. (continued)

A	B	C	D	E
2.6902(1.5)			2.681(m)	2.666(m)
2.6314(2.8)				2.512(m)
2.5829(2.9)				
2.5415(1.0)				
2.4933(2.1)				
2.4669(1.5)				
2.4485(2.0)	2.459(w)		2.426(w)	
2.3640(2.5)				
2.3513(1.0)				
2.3336(1.3)				
2.3093(2.5)	2.316(w)			2.312(m)
2.3026(1.6)			2.298(w)	
2.2635(1.1)				
2.2543(1.1)				2.254(m)
2.2347(1.6)				
2.2239(1.6)				2.208(m)
2.1874(1.8)				
2.1676(1.7)				
2.1600(1.3)				2.163(m)
2.1581(1.8)				
2.1376(2.1)				
2.1360(1.6)	2.129(m)	2.131(w)		1.958(m)

ratory, New York. For molybdenum and chlorine analyses, weighed samples were decomposed in ammonical hydrogen peroxide solutions, with heating. After acidification, the chlorine samples were titrated potentiometrically with $AgNO_3$. The molybdenum samples were acidified and precipitated with 8-hydroxyquinoline.[44] The great sensitivity of many of these materials to air made their analyses difficult. This is evidenced in the sum of all constituent elements frequently falling a few percent short of 100% (typically between 96% and 100%). C, H, and N analyses in particular indicated a loss of pyridine when the samples were exposed briefly to air. Because of this, the formulas quoted are based upon the observed ratios, and the calculated percentages have not been included.

The reaction of Mo_6Cl_{12} and NaSH in a 1:16 mole ratio at 225°C in pyridine was executed by placing 0.50 g (0.5 mmole) Mo_6Cl_{12} and 0.45 g (8.0 mmole) NaSH in a 13 mm OD reaction tube fitted with a Teflon needle valve. Approximately 10 mL of dry pyridine were distilled in the tube, and the tube was sealed off below the valve such that its length was about 15 cm. Upon warming, the resulting slurry turned red and bubbled. The tube was placed in a Parr general purpose bomb containing several mL of pyridine. The pyridine was placed in the bomb to minimize the pressure differential between the inside and outside of the reaction tube. Even

with this precaution, tubes sometimes broke. After the tube was heated at 110°C for one day, it was cooled to room temperature, removed from the bomb, shaken thoroughly and replaced. The temperature was then maintained at 225° ± 5°C for 7.8 days. Next the bomb was slowly cooled to room temperature over approximately two days, the tube was opened under a stream of nitrogen and filtered in Schlenk ware. The insoluble black powder was then ground with a mortar and pestle, and extracted with methanol for 8 days. Found for $Mo_{1.0}S_{2.3}py_{0.2}$ (py = C_5H_5N): Mo, 51.61; Cl, 0.00; C, 6.01; H, 0.83; N, 1.43.

The reaction of Mo_6Cl_{12} and NaSH in a 1:16 mole ratio was also carried out by refluxing in pyridine 1.50 g (1.5 mmole) Mo_6Cl_{12} and 1.34 g (23.9 mmole) NaSH in a Schlenk reflux flask equipped with a water cooled condenser. About 40 mL of dry pyridine were introduced, and the reaction was refluxed for 6.7 days. The solution was filtered to yield a black powder and bright red solution. The black powder was ground and extracted with methanol for about two weeks; yield 78%. This material was pyrophoric. Found for $Mo_{6.0}S_{6.5}Cl_{1.6}py_{2.8}$: Mo, 51.85; S, 18.65; Cl, 5.05; C, 15.25; H, 1.75; N, 3.59; Na, 0.24; total, 96.83%.

The reaction of Mo_6Cl_{12} and NaSH in a 1:12 mole ratio was performed by reacting 0.50 g (0.50 mmole) Mo_6Cl_{12} and 0.33 g (5.9 mmole) NaSH in ca. 40 mL of refluxing 3,5-luti-

dine for 3.7 days. The reaction products were filtered to give a brown solid and yellow solution. The brown solid was ground and extracted with methanol for four days; yield, 76%. Found for $Mo_{6.0}S_{6.2}Cl_{3.0}lut_{4.8}$ (lut = 3,5-lutidine): Mo, 40.52; S, 13.98; Cl, 7.39; C, 28.29; H, 3.11; N, 4.67; total, 97.96%.

The reaction of Mo_6Cl_{12} and NaSH in a 1:8 mole ratio was prosecuted by reacting 0.50 g (0.5 mmole) Mo_6Cl_{12} and 0.22 g (3.9 mmole) NaSH with about 10 mL of pyridine in a sealed tube at 200°C for 7.0 days. After cooling slowly to room temperature over two days, the reaction mixture was filtered to give a black powder and a dark red solution. The black powder was ground and extracted with methanol for two weeks; yield, 77%. Found for $Mo_{6.0}S_{7.1}Cl_{2.2}py_{4.9}$: Mo, 44.78; S, 17.72; Cl, 5.86; C, 22.70; H, 2.16; N, 5.94; Na, 0.06; total, 99.22%.

The reaction of Mo_6Cl_{12} and NaSH in a 1:8 mole ratio was studied by reacting 1.50 g (1.5 mmole) Mo_6Cl_{12} and 0.67 g (12.0 mmole) NaSH in refluxing 3,5- lutidine for 8.0 days. The products were filtered. A light-brown powder and brown-red solution resulted. The powder was ground and extracted for two weeks with methanol; yield, 82%. Found for $Mo_{6.0}S_{6.0}Cl_{4.2}lut_{5.0}$: Mo, 39.97; S, 13.39; Cl, 10.28; C, 29.10; H, 3.12; N, 4.77; Na, 0.39; total, 101.02%.

The reaction of Mo_6Cl_{12} and NaSH in a 1:8 mole ratio

was also studied by refluxing 1.50 g (1.5 mmole) Mo_6Cl_{12} and 0.67 g (12.0 mmole) NaSH in about 40 mL of pyridine for 6.0 days. The reaction products were filtered to yield an umber solid and a dark red solution. The solid was ground and extracted with methanol for about two weeks; yield, 58%. The product smokes when exposed to air. Found for $Mo_{6.0}S_{4.9}Cl_{4.3}py_{3.8}$: Mo, 48.45; S, 13.12; Cl, 12.89; C, 19.42; H, 1.78; N, 4.71; Na, 0.17; total, 100.54%.

The reaction of Mo_6Cl_{12}, NaSH and sulfur in a mole ratio of 1:6:2 was performed by heating 0.50 g (0.5 mmole) Mo_6Cl_{12}, 0.17 g (3.0 mmole) NaSH and 0.03 g (0.9 mmole) sulfur in 200°C pyridine in a sealed tube for 3.0 days. After cooling to room temperature over about two days, the resulting black powder was ground and extracted with methanol for 4 days; yield, 54%. Found for $Mo_{6.0}S_{9.3}Cl_{1.9}py_{4.9}$: Mo, 43.14; Cl, 5.10; C, 22.18; H, 2.04; N, 5.10%. When this reaction was repeated $Mo_{6.0}S_{9.7}Cl_{1.9}py_{5.4}$ resulted. Found: Mo, 41.42; S, 22.27; Cl, 4.80; C, 23.48; H, 2.10; N, 5.50; Na, 0.22; total, 99.79%.

The reaction of Mo_6Cl_{12}, NaSH and Na_2S in a mole ratio of 1:4:4 was prosecuted by reacting 1.50 g (1.5 mmole) Mo_6Cl_{12}, 0.34 g (6.1 mmole) NaSH and 0.47 g (6.0 mmole) Na_2S in about 40 mL of refluxing pyridine for 7.0 days. Filtering yielded chocolate-brown powder and brown-red solution. The powder was ground and extracted with methanol for about

2.5 weeks; yield, 58%. Found for $Mo_{6.0}S_{5.3}Cl_{2.4}py_{2.3}$: Mo, 45.68; S, 13.44;, Cl, 6.69; C, 23.20; H, 2.01; N, 5.40; Na, 0.63; total, 97.05%.

The reaction of Mo_6Cl_{12} and Na_2S in a 1:8 mole ratio was performed by refluxing 1.50 g (1.5 mmole) Mo_6Cl_{12} and 0.94 g (12.0 mmole) Na_2S in pyridine for 7 days. Filtration yielded a black solid which was ground and extracted with methanol for 9 days; yield, 76%. Found for $Mo_{6.0}S_{8.6}Cl_{1.2}py_{3.6}$: Mo, 46.83; S, 22.56; Cl, 3.54; C, 17.37; H, 1.59; N, 3.91; Na, 1.88; total, 97.68%.

RESULTS

Several routes of converting Mo_6Cl_{12} to $(Mo_6S_8)L_6$ were examined in this work. The reactions explored and hypothetical products are shown below:

(1) $Mo_6Cl_{12} + 16\ NaSH \xrightarrow{py} (Mo_6S_8)py_6 + 2\ H_2 + 4\ H_2S + 12\ NaCl + 4\ NaSH$

(2) $Mo_6Cl_{12} + 12\ NaSH \xrightarrow{py} (Mo_6S_8)py_6 + 2\ H_2 + 4\ H_2S + 12\ NaCl$

(3) $Mo_6Cl_{12} + 8\ NaSH \xrightarrow{py} (Mo_6S_8)py_6 + 2\ H_2 + 4\ pyH^+Cl^- + 8\ NaCl$

(4) $Mo_6Cl_{12} + 6\ NaSH + 2\ S \xrightarrow{py} (Mo_6S_8)py_6 + 6\ pyH^+Cl^- + 6\ NaCl$

(5) $Mo_6Cl_{12} + 4\ NaSH + 4\ Na_2S \xrightarrow{py} (Mo_6S_8)py_6 + 2\ H_2 + 12\ NaCl$

(6) $Mo_6Cl_{12} + 8\ Na_2S \xrightarrow{py} Na_4(Mo_6S_8)py_6 + 12\ NaCl.$

The reaction of 1 Mo_6Cl_{12}: 16 NaSH in 225°C pyridine for 7.8 days resulted in $Mo_{1.0}S_{2.3}py_{0.2}$. The x-ray powder pattern of this material differs from that of $(Mo_6X_8)py_6$ (Table III) and the cluster is probably not retained. The powder pattern does not contain lines of Mo_6S_8, Mo_2S_3 or MoS_2, and it is not clear what species comprise the bulk material. The molybdenum 3d x-ray photoelectron spectrum exhibits at least two types of molybdenum. The major components are separated by about 0.5 eV, are present in approx-

imately equal amounts, and have 3d 5/2 binding energies of 229.0 and 228.5 eV. When the formula is written as $Mo_{6.0}S_{13.8}py_{5.4}$, it is clear this material differs significantly from the other reaction products to be discussed. Apparently the reaction conditions and SH^- to Mo_6Cl_{12} ratio are sufficiently extreme to destroy the cluster.

The same reactants run in refluxing pyridine (1 Mo_6Cl_{12}: 16 NaSH, 115°C py, 6.7 days) gave rise to $Mo_{6.0}S_{6.5}Cl_{1.6}py_{2.8}$. The x-ray powder pattern (Table III) demonstrates that the $(Mo_6X_8)py_6$ structure is retained. The x-ray photoelectron spectrum exhibits a broad molybdenum 3d signal which appears to arise from one type of molybdenum (Figure 13). The peaks at 231.0, 227.8, and 225.1 eV arise from Mo 3d 3/2, Mo 3d 5/2 and S 2s states, respectively. The "+" symbols in Figure 13 represent the corrected experimental data, the solid curve through the data is the simulated spectrum, and the three curves discussed above correspond to the components resolved by the APES program. Figure 14 is the chlorine 2p x-ray photoelectron spectrum. The use of photoelectron spectroscopy to determine the proportions of bridging and terminal halides is well-established,[52,53,98] and the spectrum has been resolved into two components corresponding to bridging chlorine (2p 3/2, 199.2 eV) and terminal chlorine (2p 3/2, 197.6 eV). Each component is the sum of one 2p 3/2 and one 2p 1/2 peak. The ratio of bridging chlorine (Cl_B) to termi-

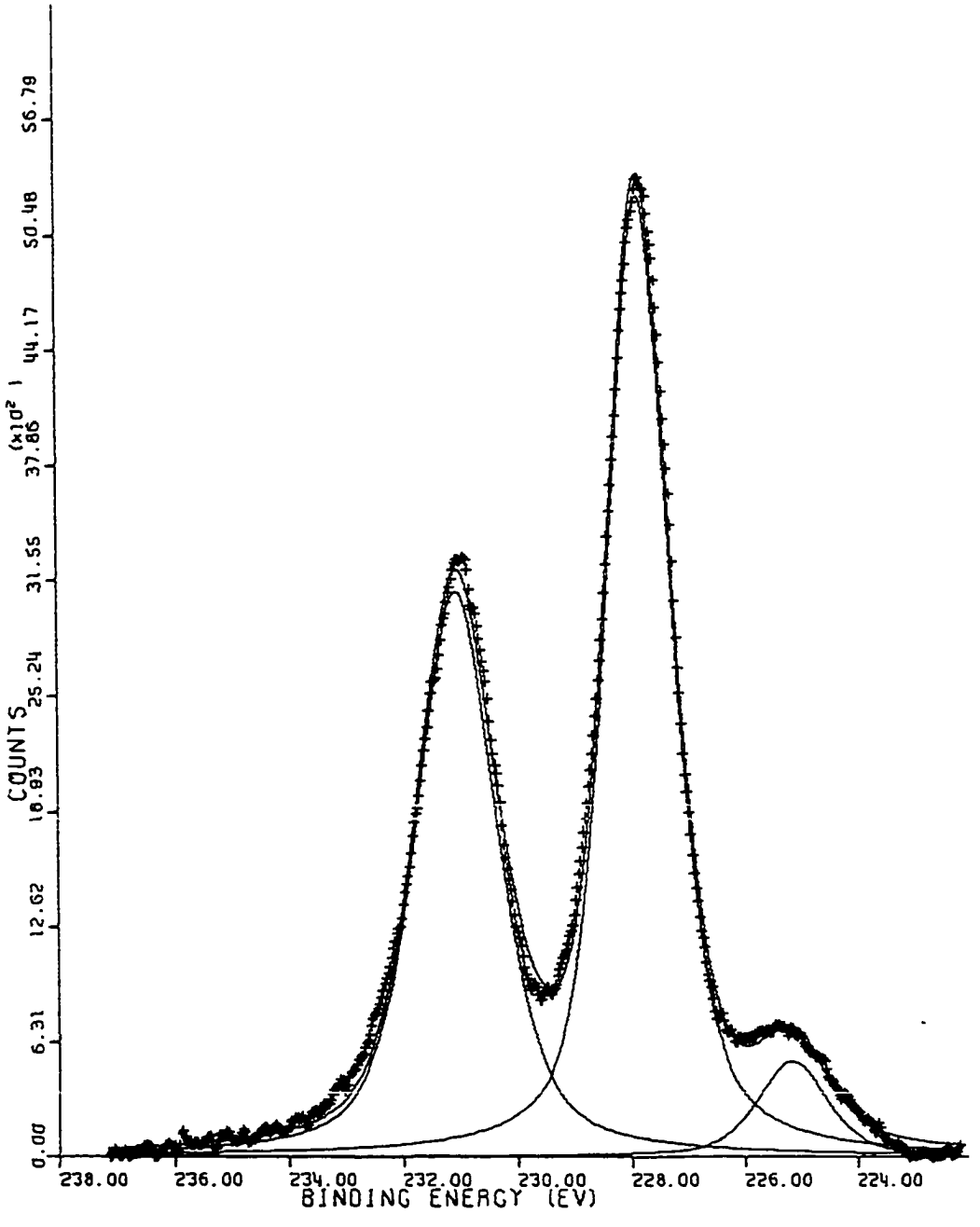

Figure 13. Molybdenum 3d x-ray photoelectron spectrum of $Mo_{6.0}S_{6.5}Cl_{1.6}py_{2.8}$

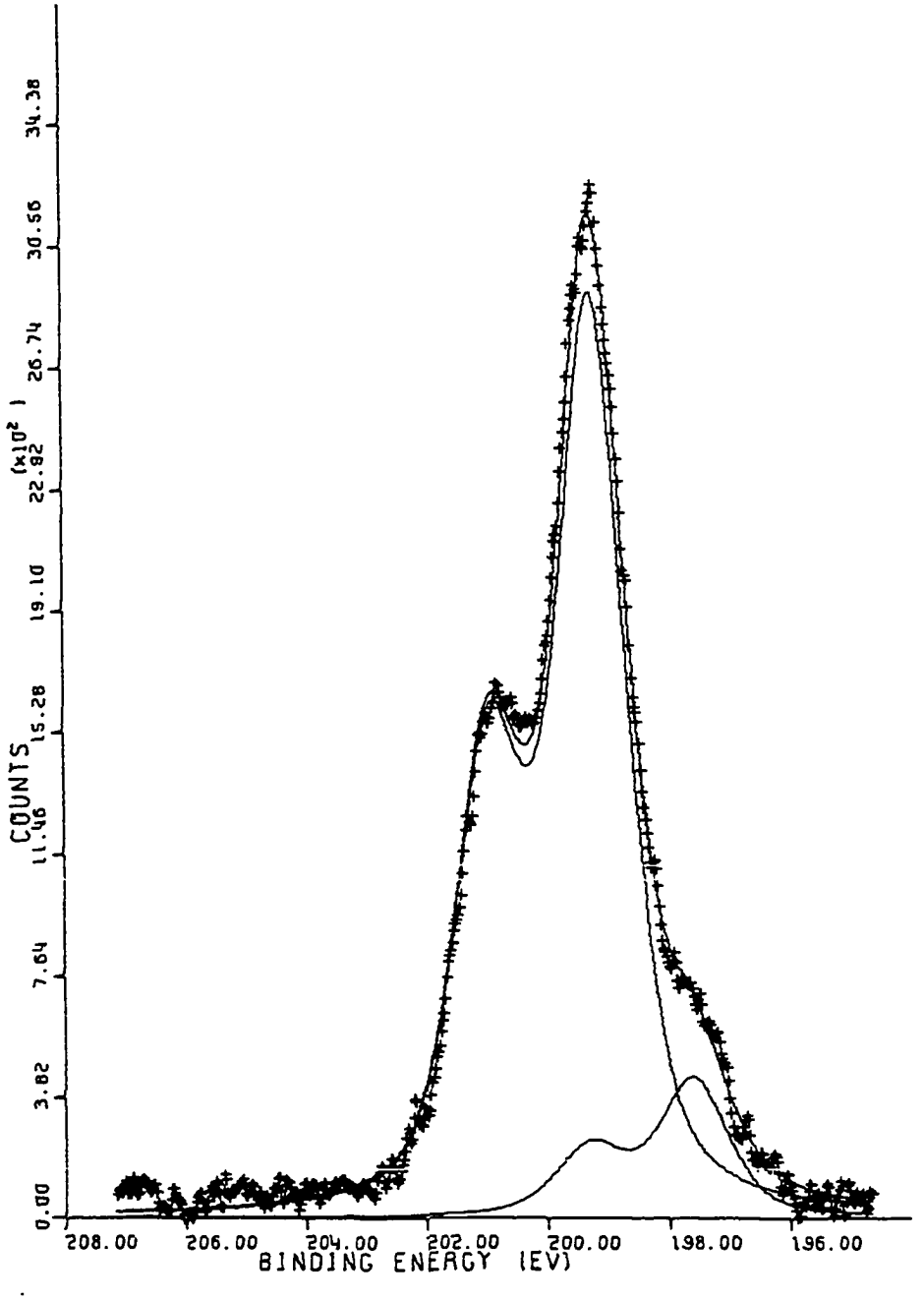

Figure 14. Chlorine 2p x-ray photoelectron spectrum of $Mo_{6.0}S_{6.5}Cl_{1.6}py_{2.8}$

nal chlorine (Cl_T) is 6.6:1.0. These data, in conjunction with elemental analyses, indicate 1.4 Cl_B and 0.2 Cl_T per Mo_6 cluster (the number of Cl_B and Cl_T per Mo_6 cluster as determined from molybdenum analysis, chlorine analysis, and least squares fitting of the x-ray photoelectron spectrum can only be considered approximate). Elemental analysis indicates 0.24% sodium is present in $Mo_{6.0}S_{6.5}Cl_{1.6}py_{2.8}$. This is probably present as NaCl which was not completely removed from the product. Ionic chlorine, corresponding to this NaCl, is found at lower binding energy than terminal chlorine is found. Ionic chlorine does not appear to make a significant contribution to the chlorine x-ray photoelectron spectrum in Figure 14. The peak at 197.6 eV is about twice as intense as would be expected for ionic chlorine based on the amount of sodium present. One of the small protuberancies at low binding energy in Figure 14 may correspond to the small amount of ionic chlorine present. Figure 15 exhibits the sulfur 2p x-ray photoelectron spectrum of this compound fit by two kinds of sulfur. The large full-width at half-maximum (FWHM) of this spectrum seemed to indicate the presence of two types of sulfur in analogy to the chlorine spectrum. The ensuing analysis yielded a bridging 2p 3/2 peak at 161.8 eV and a terminal 2p 3/2 peak at 160.8 eV with 5.1 S_T and 1.4 S_B per Mo_6 cluster. Using these data, there are only 2.8 total bridging ligands and 8.1 terminal ligands

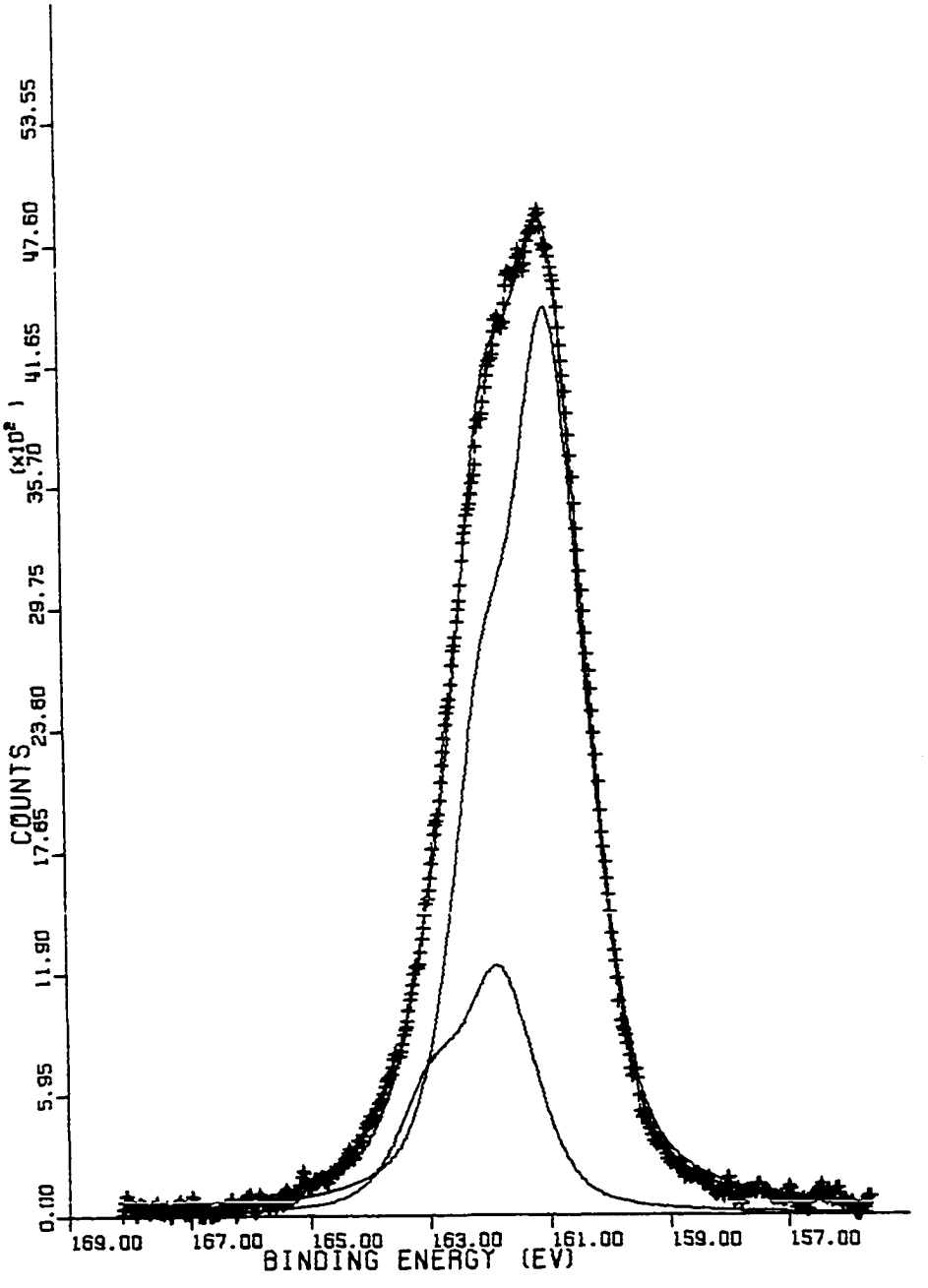

Figure 15. Sulfur 2p x-ray photoelectron spectrum of $Mo_{6.0}S_{6.5}Cl_{1.6}py_{2.8}$ fit by two types of sulfur

(including pyridine) in obvious discord with the expected 8 bridging and 6 terminal ligands required by the $(Mo_6X_8)L_6$ cluster. The x-ray powder diffraction pattern indicates the $(Mo_6X_8)L_6$ unit, or at least a very similar cluster, is present; therefore, this interpretation of the x-ray photoelectron spectrum probably is not correct. A more reasonable explanation is to consider the sulfur spectrum as arising solely from bridging sulfurs. The total number of bridging and terminal ligands is then 7.9 and 3.0, respectively. Figure 16 shows the x-ray photoelectron spectrum fit with one type of sulfur and Table IV summarizes the x-ray photoelectron data. Since the spin-orbit separation is on the order of the FWHM, only a single asymmetric peak is observed.

An anomalous feature of these spectra is the rather large full-width at half-maximum they exhibit: the Mo 3d 5/2 peak in this compound has a FWHM of 1.36 eV while that of the S 2p 3/2 peak is 1.62 eV. The corresponding values in MoS_2 measured under similar conditions are 1.10 and 1.21 eV, respectively. Broad peaks are probably observed because the spectra are caused by many quite similar atoms rather than a single, well-defined type of atom. Consider the 6.5 sulfur atoms in the present case: some clusters must have only six sulfurs while others will have seven. In reality, some clusters may even have eight sulfurs and others perhaps five or fewer. This range of bridging atoms would give rise to many

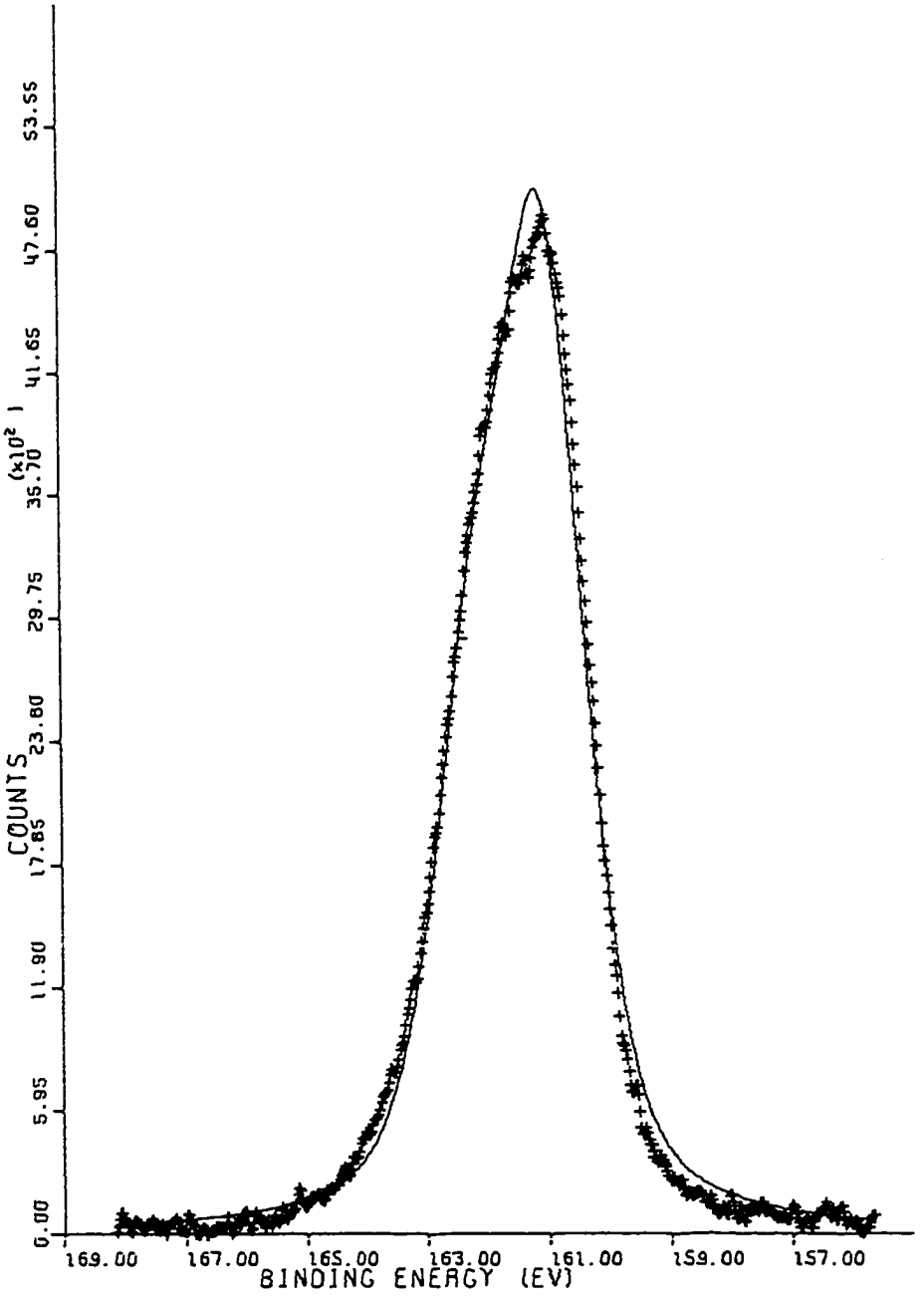

Figure 16. Sulfur 2p x-ray photoelectron spectrum of $Mo_{6.0}S_{6.5}Cl_{1.6}py_{2.8}$ fit by one type of sulfur

Table IV. X-ray photoelectron data[a]

Sample	Mo 3d 5/2	Cl_B 2p 3/2	Cl_T 2p 3/2	S 2p 3/2
$Mo_{1.0}S_{2.3}py_{0.2}$[b]	228.5(1.75)	-	-	161.7(1.70)
	229.0			
$(Mo_{6.0}S_{6.5}Cl_{1.4})Cl_{0.2}py_{2.8}$[c]	227.8(1.36)	199.2(1.36)	197.6(1.36)	161.0(1.62)
$(Mo_{6.0}S_{6.2}Cl_{2.5})Cl_{0.5}lut_{4.8}$[d]	227.8(1.45)	199.2(1.40)	197.4(1.40)	161.0(1.85)
$(Mo_{6.0}S_{7.1}Cl_{0.5})Cl_{1.7}py_{4.9}$[e]	228.1(1.62)	199.2(1.65)	197.6(1.72)	161.3(1.72)
$(Mo_{6.0}S_{6.0}Cl_{3.5})Cl_{0.7}lut_{5.0}$[f]	228.1(1.44)	199.4(1.41)	197.2(1.41)	161.1(1.76)
$(Mo_{6.0}S_{4.9}Cl_{3.6})Cl_{0.7}py_{3.8}$[g]	228.0(1.41)	199.5(1.43)	197.6(1.43)	161.2(1.80)

[a]All binding energies and FWHM's are in eV. FWHM are given in parentheses.

[b]Product of 1 Mo_6Cl_{12} and 16 NaSH in 225°C pyridine for 7.8 days.

[c]Product of 1 Mo_6Cl_{12} and 16 NaSH in 115°C pyridine for 6.7 days.

[d]Product of 1 Mo_6Cl_{12} and 12 NaSH in 170°C 3,5-lutidine for 3.7 days.

[e]Product of 1 Mo_6Cl_{12} and 8 NaSH in 200°C pyridine for 7.0 days.

[f]Product of 1 Mo_6Cl_{12} and 8 NaSH in 170°C 3,5-lutidine for 8.0 days.

[g]Product of 1 Mo_6Cl_{12} and 8 NaSH in 115°C pyridine for 6.0 days.

Table IV. (continued)

Sample	Mo 3d 5/2	Cl_B 2p 3/2	Cl_T 2p 3/2	S 2p 3/2
$Mo_{6.0}S_{9.3}Cl_{1.9}py_{4.9}$ [h]	228.4(1.47)	-	-	161.4(1.70)
$(Mo_{6.0}S_{9.7}Cl_{0.7})Cl_{1.2}py_{5.4}$ [i]	228.4(1.50)	199.3(1.65)	197.5(1.65)	161.4(1.74)
$(Mo_{6.0}S_{5.3}Cl_{1.9})Cl_{0.5}py_{2.3}$ [j]	227.8(1.56)	199.3(1.44)	197.7(1.44)	160.8(1.70)
$Na(Mo_{6.0}S_{8.6}Cl_{0.9})Cl_{0.3}py_{3.6}$ [k]	227.8(1.65)	199.3(1.55)	197.9(1.55)	161.0(1.76)

[h] Product of 1 Mo_6Cl_{12}, 6 NaSH and 2 S in 200°C pyridine for 3.0 days.

[i] Product of 1 Mo_6Cl_{12}, 6 NaSH and 2 S in 200°C pyridine for 3.0 days

[j] Product of 1 Mo_6Cl_{12}, 4 NaSH and 4 Na_2S in 115°C pyridine for 7.0 days.

[k] Product of 1 Mo_6Cl_{12} and 8 Na_2S in 115°C pyridine for 7.0 days.

different molybdenum environments, all possessing slightly different binding energies, thus a broadened molybdenum peak is observed. The sulfur and chlorine atoms would also experience slightly different environments and give rise to broad peaks. Therefore, the best description of the bulk material is $(Mo_{6.0}S_{6.5}Cl_{1.4})Cl_{0.2}py_{2.8}$. These data are not accurate enough to address the question of the cluster being deficient in bridging ligands. However, the cluster appears to be truly deficient in terminal ligands and this will be discussed shortly. This formulation would predict approximately 21.4 cluster electrons, and it is curious that no room temperature ESR spectrum is observed. Figure 17b shows the infrared spectrum of $(Mo_{6.0}S_{6.5}Cl_{1.4})Cl_{0.2}py_{2.8}$. The peak at 431 cm^{-1} is due to coordinated pyridine, but mixing of the Mo-Cl and Mo-S modes excludes specific assignments for the other major peaks.[98]

A previously reported[98] reaction of sixteen equivalents of NaSH with one equivalent of Mo_6Cl_{12} in refluxing pyridine for only 12 to 14 hours produced $Mo_{6.0}S_{5.4}Cl_{3.0}py_{2.9}$. It would appear that sulfur initially substitutes into the cluster rapidly, but slows as the substitution becomes more extensive.

The reaction of Mo_6Cl_{12} and NaSH in a 1:12 mole ratio in refluxing 3,5-lutidine produced $Mo_{6.0}S_{6.2}Cl_{3.0}(lut)_{4.8}$. Its x-ray diffraction powder pattern naturally differs from

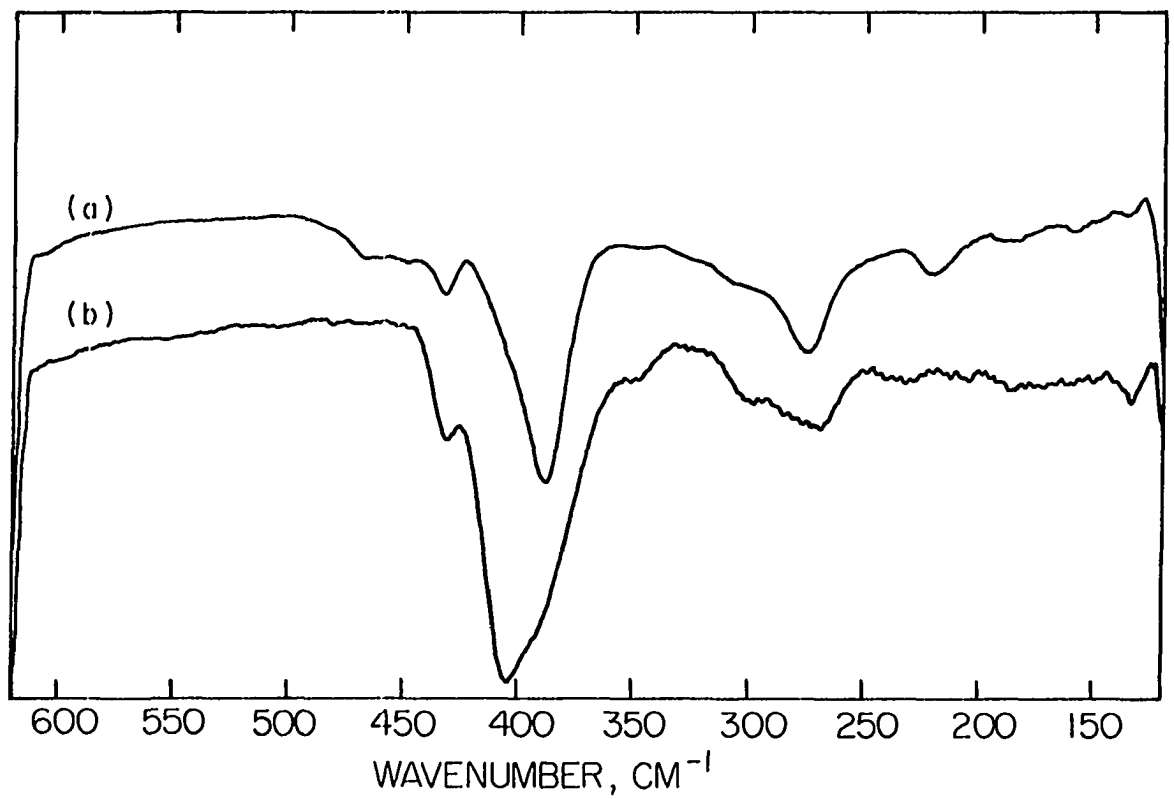

Figure 17. Infrared spectra of $(Mo_{6.0}S_{7.1}Cl_{0.5})Cl_{1.7}py_{4.9}$, a; $(Mo_{6.0}S_{6.5}Cl_{1.4})Cl_{0.2}py_{2.8}$, b

that of $(Mo_6X_8)py_6$, but it seems reasonable to assume the cluster is retained under these conditions. X-ray photoelectron spectra indicate the formulation should be $(Mo_{6.0}S_{6.2}Cl_{2.5})Cl_{0.5}(lut)_{4.8}$. This material gave no ESR signal.

The reaction of 1 equivalent of Mo_6Cl_{12} with 8 equivalents of NaSH in 200°C pyridine produced $Mo_{6.0}S_{7.1}Cl_{2.2}py_{4.9}$. The x-ray powder pattern showed the $(Mo_6X_8)L_6$ cluster was retained and the x-ray photoelectron data indicate the formula $(Mo_{6.0}S_{7.1}Cl_{0.5})Cl_{1.7}py_{4.9}$. It should be noted that this compound has significantly more Cl_T than Cl_B. Figure 18 shows the chlorine 2p photoelectron spectrum of this compound and Figure 17a shows the infrared spectrum. The major difference between the infrared spectrum of this material and that of $(Mo_{6.0}S_{6.5}Cl_{1.4})Cl_{0.2}py_{2.8}$ is the change in the large peak near 400 cm^{-1}. The spectrum of $(Mo_{6.0}S_{7.1}Cl_{0.5})Cl_{1.7}py_{4.9}$ has an intense peak at 386 cm^{-1} with a shoulder at 403 cm^{-1}. The intensities are reversed in $(Mo_{6.0}S_{6.5}Cl_{1.4})Cl_{0.2}py_{2.8}$: there is an intense peak at 406 cm^{-1} and a shoulder at 385 cm^{-1}. This inversion of intensities corresponds to a major change in the ratio of Cl_B to Cl_T and a change in the number of sulfurs per cluster. The very weak signal observed in the ESR spectrum may be due to an impurity.

When the 1 Mo_6Cl_{12} : 8 NaSH reaction was run in 3,5-lutidine the product analyzed as $Mo_{6.0}S_{6.0}Cl_{4.2}lut_{5.0}$. Its x-

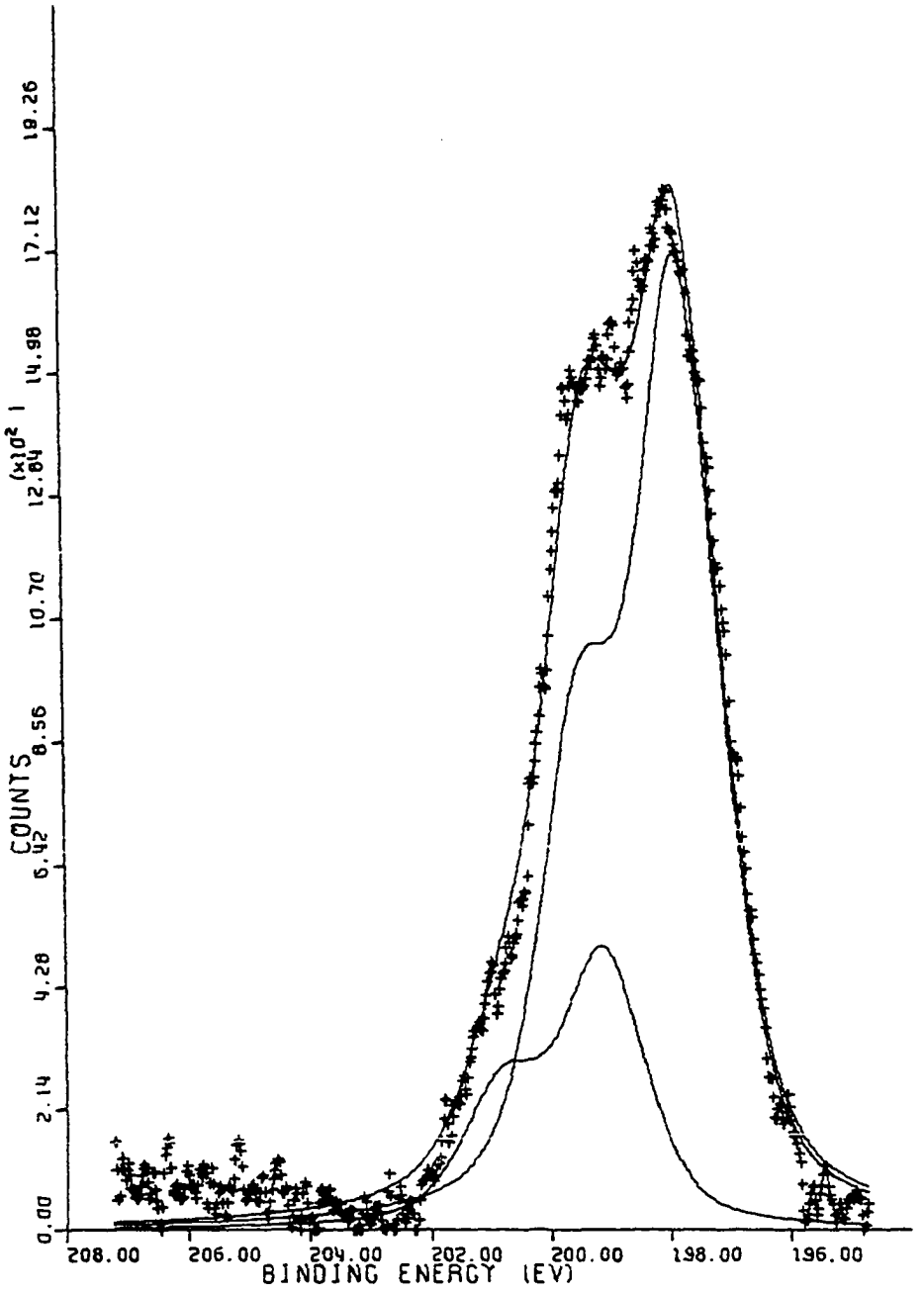

Figure 18. Chlorine 2p x-ray photoelectron spectrum of $Mo_{6.0}S_{7.1}Cl_{2.2}py_{4.9}$

ray powder pattern matched that of $(Mo_{6.0}S_{6.2}Cl_{2.5})Cl_{0.5}$ $lut_{4.8}$ (the 1 Mo_6Cl_{12} : 12 NaSH, 170°C lut, 3.7 day reaction), and the x-ray photoelectron spectrum indicates the formulation $(Mo_{6.0}S_{6.0}Cl_{3.5})Cl_{0.7}lut_{5.0}$ is in order. No room temperature ESR spectrum was observed for this material.

The 1 Mo_6Cl_{12} : 8 NaSH reaction run in refluxing pyridine yielded $Mo_{6.0}S_{4.9}Cl_{4.3}py_{3.8}$ which is written as $(Mo_{6.0}S_{4.9}Cl_{3.6})Cl_{0.7}py_{3.8}$ because of the x-ray photoelectron data. The x-ray diffraction powder pattern of this material exhibits only three very diffuse lines, and the sample is considered amorphous.

The 1 Mo_6Cl_{12} : 6 NaSH : 2 S reaction, run twice at 200°C, yielded slightly different products. This may be due to slight inaccuracies in weighing and transferring reactants, but undoubtedly is based largely on insufficient mixing of reactants in the tubes during heating. Long reaction times should help minimize this problem. The products are $Mo_{6.0}S_{9.3}Cl_{1.9}py_{4.9}$ and $Mo_{6.0}S_{9.7}Cl_{1.9}py_{5.4}$. The x-ray powder pattern demonstrates the cluster is retained and x-ray photoelectron data indicate the latter should be formulated as $(Mo_{6.0}S_{9.7}Cl_{0.7})Cl_{1.2}py_{5.4}$. These formulas indicate excess sulfur is present, although it is not clear in what species it is contained. Both compounds gave identical, weak ESR spectra.

The 1 Mo_6Cl_{12} : 4 NaSH : 4 Na_2S reaction run in reflux-

ing pyridine produced $Mo_{6.0}S_{5.3}Cl_{2.4}py_{2.3}$. The cluster is retained, as judged from the x-ray powder pattern, and the x-ray photoelectron spectrum indicates the correct formulation is $(Mo_{6.0}S_{5.3}Cl_{1.9})Cl_{0.5}py_{2.3}$. No room temperature ESR spectrum was observed.

The 1 Mo_6Cl_{12} : 8 Na_2S reaction was run in refluxing pyridine and produced $Na_{1.0}Mo_{6.0}S_{8.6}Cl_{1.2}py_{3.6}$. The x-ray powder pattern is of significantly lower quality than those of the other products, but it does indicate the cluster is retained. The x-ray photoelectron data indicate this compound should be formulated as $Na_{1.0}(Mo_{6.0}S_{8.6}Cl_{0.9})Cl_{0.3}py_{3.6}$. There is no evidence of NaCl being present and no ESR spectrum is observed at room temperature.

DISCUSSION

The reaction products described in this study exhibit certain trends. It is possible to make materials of the type $(Mo_6S_{8-x}Cl_x)Cl_ypy_z$ where $0 \leq x \leq 7$ and $y + z \leq 6$ by several different methods. All of the procedures investigated involve substituting sulfur for bridging chlorine in Mo_6Cl_{12}. Judging from the similarity of the products' x-ray diffraction powder patterns to that of $(Mo_6X_8)py_6$, the products contain isolated Mo_6 clusters with no inter-cluster bonding. The amount of sulfur contained in the product increases with increasing reaction time, increasing reaction temperature, and when NaSH is a reactant, increasing amount of starting sulfur reagent. High temperatures and large excesses of sulfur reagent, as in the 1 Mo_6Cl_{12} : 16 NaSH reaction at 225°C, are capable of destroying the cluster. The same reaction run under the less vigorous conditions of refluxing pyridine left the cluster intact.

Stoichiometric amounts of NaSH at low temperatures, as in the 1 Mo_6Cl_{12} : 8 NaSH reaction done in refluxing pyridine, yield amorphous products. Under the relatively mild conditions employed, it seems unlikely that the Mo_6 cluster is destroyed. Crystalline material results from the higher temperature reactions of 1 Mo_6Cl_{12} : 8 NaSH in either refluxing 3,5-lutidine or 200°C pyridine, as well as the low

temperature reaction of Mo_6Cl_{12} with excess NaSH (1 Mo_6Cl_{12} : 16 NaSH) in refluxing pyridine. Apparently, there exists a critical temperature, critical reaction ratio, or critical reaction time before well-formed, isolated Mo_6 clusters are formed. These critical conditions are more vigorous than the reaction conditions required to substitute some sulfur atoms into bridging positions.

The exact nature of the reaction products is not known, but the unexpected amorphousness of $(Mo_{6.0}S_{4.9}Cl_{3.6})Cl_{0.7}py_{3.8}$ (1 Mo_6Cl_{12} : 8 NaSH in refluxing pyridine) suggests a general reaction path. It is known that 1 equivalent of Mo_6Cl_{12} reacts readily with two equivalents of SH^- to form pyridine soluble $(Mo_6Cl_7S)Cl_3py_3$.[98] Furthermore, as the degree of sulfur substitution increases, the products become increasingly insoluble in pyridine. It is now proposed that the reaction of Mo_6Cl_{12} with 8 or more equivalents of SH^- quickly forms clusters low in sulfur like $(Mo_6Cl_7S)^{3+}$ or $(Mo_6Cl_6S_2)^{2+}$. Increasing substitution of sulfur causes the formation of insoluble intermediates which are poorly formed amorphous materials. In the case of $(Mo_{6.0}S_{4.9}Cl_{3.6})Cl_{0.7}py_{3.8}$ (1 Mo_6Cl_{12} : 8 NaSH in refluxing pyridine), the reaction conditions are not sufficiently severe to form a crystalline product, and the product is instead the amorphous "intermediate".

The nature of the amorphous material can be profitably

speculated upon. As the Mo_6 clusters are quite likely intact, the disorder is either due to the partial absence of terminal ligands in the clusters or the random linkage of clusters. The absence of some terminal ligands could conceivably favor the formation of inter-cluster bridges. Such bridging would replace the terminal pyridine ligands with bridging chlorine, or possibly sulfur atoms, and the resulting materials with randomly missing terminal ligands and randomly occurring bridges would probably be amorphous. $(Mo_{6.0}S_{4.9}Cl_{3.6})Cl_{0.7}$ $py_{3.8}$ (1 Mo_6Cl_{12} : 8 NaSH in refluxing pyridine) exhibits a deficiency of terminal ligands as would be expected from such inter-cluster bridging. A material with randomly missing ligands or randomly coupled clusters would also have a dispersion of similar, yet distinct, atomic environments. Such a dispersion would engender the large full-widths at half-maximum which the x-ray photoelectron spectra display.

The crystalline products have the $(Mo_6X_8)L_6$ structure. The analytical data generally indicate non-stoichiometric products, but it is not known if the sulfur and chlorine are dispersed in a solid solution or if the bulk material is a mixture of similar, yet distinct compounds like $(Mo_6S_8)L_6$, $(Mo_6S_7Cl)L_6$, $(Mo_6S_6Cl_2)L_6$ and others. The distinction is primarily based upon the distribution of ligands. A solid solution would have a statistical distribution of ligands and would be a fairly homogeneous sample. A mixture would be a

more complicated case and might have equal amounts of several compounds present or even have specific members missing. Knowing the distribution of ligands in the materials would assist in formulating a reaction mechanism, but such information is not available.

The ratios of bridging and terminal chlorines seen in the x-ray photoelectron spectra are puzzling. Previous work on $(Mo_6S_6Cl_2)py_6$ did not indicate any terminal halides,[98] yet terminal chlorine atoms are quite evident in the present study (Figures 14 and 18) and show no systematic variation between products. It may be the sulfur substitution occurs by a sulfur replacing a terminal chlorine, followed by exchange with a bridging chlorine. This process would yield significant numbers of terminal chlorines which may only be slowly lost and replaced by pyridine ligands.

The full complement of terminal pyridine ligands present in $(Mo_6S_6Cl_2)py_6$ renders the deficiency of terminal ligands in the present study anomalous. The Mo-N bonds of $(Mo_6S_6Cl_2)py_6$ average 2.29(2)Å which are fairly long.[98] The pyridine rings in $(Mo_6S_6Cl_2)py_6$ have large thermal parameters and two of the rings could only be refined isotropically. The occupancy of these rings was not refined in the single crystal x-ray structure determination, but a difference Fourier synthesis did not indicate pyridine deficiencies.

It is not known at what stage of the synthesis the pyr-

idine deficiency arises. The low pyridine-to-Mo_6 ratio could result from precursor clusters which are interlinked through Mo-S-Mo or Mo-Cl-Mo bonds that are converted slowly or not at all to the $(Mo_6X_8)py_6$ structure. Alternatively, pyridine could be lost from the $(Mo_6X_8)py_6$ cluster late in the reaction scheme to give a pyridine deficient product. Some pyridine may also be lost during the methanol extraction or vacuum drying stages. Some pyridine in the present study is lost upon brief exposure to air. The terminal pyridine ligands are weakly bound and may only be retained in sufficient numbers to maintain isolated clusters.

An alternate interpretation of the data for the crystalline products indicates the products may actually be mixtures of crystalline and amorphous materials. The description of the products as discrete clusters which contain terminal chlorine ligands and are deficient in terminal pyridine ligands presupposes such clusters would display x-ray powder diffraction patterns identical to that of $(Mo_6S_6Cl_2)py_6$. If clusters deficient in terminal ligands yield an x-ray powder pattern different than the fully ligated compound, the products studied must be a mixture of $(Mo_6X_8)L_6$ and an amorphous material where X is predominantly sulfur. In this description, the x-ray powder pattern is due to the portion of the product which is crystalline, $(Mo_6X_8)L_6$, and the remainder of the sample is amorphous and does not contribute to the powder

pattern. The amorphous portion of the product would quite likely be related to the amorphous product of the 1 Mo_6Cl_{12} : 8 NaSH reaction in refluxing pyridine. Such a description would explain the deficiency of terminal ligands through inter-cluster bridges. If the products are mixtures, the formulas proposed would not be valid and the only procedure for accurately determining the compositions of the components would be to perform a separation. Attempts to separate any mixtures which may be present have been unsuccessful. Formulas proposed for the products which are greatly different from $(Mo_6X_8)L_6$ would also indicate the presence of a mixture. Such formulas include $(Mo_{6.0}S_{6.0}Cl_{3.5})Cl_{0.7}lut_{5.0}$ (1 Mo_6Cl_{12} : 8 NaSH in refluxing lutidine for 8.0 days), $(Mo_{6.0}S_{9.7}Cl_{0.7})Cl_{1.2}py_{5.4}$ (1 Mo_6Cl_{12} : 6 NaSH : 2 S, 200°C pyridine for 3.0 days), and $Na(Mo_{6.0}S_{8.6}Cl_{0.9})Cl_{0.3}py_{3.6}$ (1 Mo_6Cl_{12} : 8 Na_2S, 115°C pyridine for 7.0 days).

This work verifies that it is possible to insert sulfur into the bridging position of Mo_6Cl_{12} and form isolated clusters by the methods described. The chemistry involved and the products formed are complex. The difficulty in controlling the degree of sulfur substitution, in effecting complete sulfur substitution and the possible formation of mixtures do not make these procedures practical for the synthesis of pure $(Mo_6S_8)L_6$.

SUMMARY

Earlier workers noted the formation of a black product when Cs_3MoWCl_8H was reacted with zinc in refluxing pyridine.[41] An analogous reaction occurs between the isostructural $Cs_3Mo_2Cl_8H$ and zinc in pyridine. This work attempted to characterize the product of the $Cs_3Mo_2Cl_8H$ reaction by a variety of techniques.

If one equivalent of $Cs_3Mo_2Cl_8H$ is refluxed in pyridine with nine equivalents of zinc, a black solution results which can be evaporated to yield a black solid. Washing this solid with concentrated hydrochloric acid produces $Mo_{1.0}Cl_{1.1}py_{0.8}$. The product consists of a black powder of particles between 1 and 200 microns in size. The particles are irregular in shape, have no angularity which would indicate crystallinity, and are amorphous to both x-ray and electron diffraction. The infrared spectrum shows the presence of coordinated pyridine and chlorine. X-ray photoelectron spectroscopy indicates terminal and bridging chlorines are present in the ratio of 1.5 : 1.0 and that only one type of molybdenum is present. $Mo_{1.0}Cl_{1.1}py_{0.8}$ is very stable at elevated temperatures and can be heated for 26 hours at 300° C with little change in composition.

The chemically determined oxidation state of molybdenum in $Mo_{1.0}Cl_{1.1}py_{0.8}$ is typically 0.5+. A model to explain

the unusual oxidation state of this material based on the presence of molybdenum metal has been shown to be incorrect. The presence of a hydride might result in such an anomalous oxidation state, but combined rotation and multiple pulse NMR spectroscopy and infrared spectroscopy have failed to demonstrate the presence of a hydride.

The amorphous nature of $Mo_{1.0}Cl_{1.1}py_{0.8}$ makes a diffraction structure determination impossible. The low ligand to metal ratio indicates a highly bridged, metal-metal bonded cluster or polymer. The thermal stability and insolubility in most solvents support the polymeric or extended structure. Finally, $Mo_{1.0}Cl_{1.1}py_{0.8}$ does not appear to be a mixture of distinct compounds although the presence of a mixture of closely related compounds or a solid solution can not be eliminated.

A low temperature synthesis of Mo_6S_8 type compounds would be a valuable procedure offering advantages over the currently employed high temperature (1000°C - 1200°C) methods. One rational approach to this problem recognizes the structural similarities between the Mo_6X_8 units present in Mo_6Cl_{12} and Mo_6S_8, and attempts to substitute the bridging chlorines of Mo_6Cl_{12} with sulfur. Reactions were studied between Mo_6Cl_{12} and various combinations of sulfur containing reagents: NaSH; NaSH and sulfur; NaSH and Na_2S; and Na_2S.

If Mo_6Cl_{12} is reacted in 225°C pyridine with 16 equivalents of NaSH, the Mo_6X_8 cluster is destroyed. The reaction of Mo_6Cl_{12} with 8 equivalents of NaSH in refluxing pyridine yields an amorphous material. Intermediate proportions of NaSH at temperatures between 115°C and 200°C yield crystalline products which have x-ray diffraction powder patterns identical to those exhibited by $(Mo_6X_8)L_6$ (X = S, Cl). The formulas for the $(Mo_6X_8)L_6$ products actually have between 7.5 and 9.5 bridging ligands and between 3.0 and 5.7 terminal ligands. The deviation of the formulas from $(Mo_6X_8)L_6$ is due in part to errors in elemental analysis, curve fitting of the x-ray photoelectron spectra, and the presence of impurities. Some inter-cluster links in the impurities may contribute to the small number of terminal ligands.

It is not possible from this work to conclude if the isolated materials are solid solutions of $(Mo_6X_8)L_6$ or if they are mixtures of isolated $(Mo_6X_8)L_6$ units and amorphous intermediate materials. Either case could give rise to the non-stoichiometric formulas observed. Formulas which indicate significant differences from 6 terminal and 8 bridging ligands probably contain side-product impurities.

This work verifies the possibility of substituting S for Cl in Mo_6Cl_{12} clusters to produce $(Mo_6X_8)L_6$ clusters. The degree of sulfur substitution is difficult to control and the wanted products may be contaminated with unwanted side-

products. These disadvantages do not make the methods outlined attractive for the synthesis of $(Mo_6X_8)L_6$ compounds.

APPENDIX: APES PROGRAM

Intoduction

Photoelectron spectroscopy (PES) is a technique which measures the energy distribution of electrons in both atoms and molecules. PES, especially x-ray induced photoelectron spectroscopy, has been an important tool for structural studies from its earliest days.[102] For example, Best and Walton[103] have recently examined a wide variety of transition metal halide cluster spectra and determined it is frequently possible to distinguish terminal and bridging halides. PES is capable of giving structural insight because the energy of a bound electron depends on the chemical environment of the atom. This binding energy varies from one chemical environment to another, so that peaks in a PES spectrum due to structurally non-equivalent atoms of an element can sometimes be distinguished. Different methods for resolving an observed, complex PES spectrum into its components have been used to aid in structural interpretation. Some methods used are the following: Subtracting the spectrum of a suspected component from a complex, observed spectrum;[104] estimating components using a Du Pont 310 Curve resolver;[105,106] and fitting components to an observed spectrum by computer.[107,108] The computer program APES (Analyzed Photoelectron Spectra) smooths the PES data, adjusts the baseline

of the spectrum, corrects for inelastic electron scattering, and fits a user controlled number of components to the corrected spectrum using the method of non-linear least squares. It should be stressed that the method of non-linear least squares results in a non-unique solution. Even though a fit may appear to be excellent, the user should make use of all known chemical and physical information to review the solution.

Method

Typically, when spectra of compounds to be analyzed are being recorded, the spectrum of a standard compound is also obtained. The standard compound should ideally be one in which the element under investigation is present in a chemically similar environment and all atoms of that element are structurally equivalent. The spectrum of the standard should be obtained under instrumental conditions identical to those with which the unknowns were collected. Standard compound spectra are used to obtain reasonable values for the full-widths at half-maximum (FWHMs) and relative areas of spin-orbit split peaks (if present) as well as typical binding energies.

After a spectrum has been digitized and read into APES, a smoothing routine is executed. Two consecutive smoothings over three adjacent points are performed using

$$Y_{SMTH}(I) = \tfrac{1}{4}\left[Y(I-1) + 2Y(I) + Y(I+1)\right] \quad (1)$$

where $Y_{SMTH}(I)$ is the value of the smoothed Ith data point. Y(I) is the raw Ith data point while Y(I-1) and Y(I+1) are respectively the data points before and after Y(I).

Next, the baseline is adjusted to zero at its minimum value using

$$Y_{BASE}(I) = Y_{SMTH}(I) - B \quad (2)$$

where B equals the smallest $Y_{SMTH}(I)$ value and $Y_{BASE}(I)$ is the Ith baseline corrected point.

Finally a correction is made for inelastic electron scattering. If a PES spectrum has a constant level baseline at binding energies lower than the spectral peak(s) as well as a constant, yet higher level baseline, at higher binding energies, then the following correction[109] is made:

$$Y_{COR}(I) = Y_{BASE}(I) - K\left[\left(\sum_{N>I}^{NPTS} Y_{BASE}(N)\right)/\left(\sum_{I>1}^{NPTS} Y_{BASE}(I)\right)\right] \quad (3)$$

where $Y_{COR}(I)$ is the inelastically scattered corrected data and NPTS is the number of data points. K is defined by

$$K = k\left[Y_{BASE}(min1) - Y_{BASE}(min2)\right] \quad (4)$$

where $Y_{BASE}(min1)$ and $Y_{BASE}(min2)$ are the minimum values of Y_{BASE} in the first and last 10% of the data points, respectively, and k has been fixed to 0.03. Equation (3) is iterated several times changing $Y_{BASE}(I)$ after each iteration to the most recent $Y_{COR}(I)$ and calculating a new $Y_{COR}(I)$. K

maintains the same value in each iteration. The cycle stops when $Y_{COR}(min1)$ is less than or equal to $Y_{COR}(min2)$. Should a value of $Y_{COR}(I)$ become negative, it is set to zero. This correction assumes the difference in baseline, before and after a peak, is due completely to inelastically scattered electrons. As long as this assumption is valid the correction seems to work well.

After the inelastic scattering correction is made, the data are ready to be fit by non-linear least squares. The least squares subprogram[110] is based on the Marquardt algorithm[111] which is a combination of a gradient search and an expansion of the fitting function.

The fitting function used is

$$Y_{CALC}(I) = \sum_{a=1}^{NNEQ} Y_a(I) \qquad (5)$$

where Y_{CALC} is the synthetic spectrum and NNEQ is the suspected number of nonequivalent atoms of the element under study. $Y_a(I)$ is a combination of Gaussian and Cauchy functions

$$Y_a(I) = f\left[Y_{o,a}\exp(-(\ln 2)(X(I)-X_{o,a})^2/\Gamma_{\frac{1}{2},a}^2)\right] + (1-f)\left[(Y_{o,a}\cdot\Gamma_{\frac{1}{2},a}^2)/(\Gamma_{\frac{1}{2},a}^2 + (X(I)-X_{o,a})^2)\right]$$

$$o \leq f \leq 1 \qquad (6)$$

where $Y_a(I)$ is the calculated PES peak for the Ith point of atom type a, f is the fraction Gaussian of Y_a, $Y_{o,a}$ is the

peak height, $X_{o,a}$ is the peak position, and $\Gamma_{\frac{1}{2},a}$ is the half-width at half-maximum (HWHM) of the peak.[112] If f is kept constant, equation (6) has three variables per atom type. Figure 19 shows Y_a with f = 0.0, 0.5, and 1.0.

When spin-orbit splitting is a factor, equation (7) can be used

$$(Y_a(I))_{TOTAL} = (Y_a(I))_{LOW} + (Y_a(I))_{HIGH} \tag{7}$$

where $Y_a(I)_{LOW}$ and $Y_a(I)_{HIGH}$ represent the low binding energy spin-orbit component and high binding energy spin-orbit component, respectively. In order to reduce the number of variables in equation (7), the following relationships are used:

$$\begin{aligned} (Y_o)_{HIGH} &= c_1(Y_o)_{LOW} \\ (X_o)_{HIGH} &= (X_o)_{LOW} + X_{SOS} \\ (\Gamma_{\frac{1}{2}})_{HIGH} &= c_2(\Gamma_{\frac{1}{2}})_{LOW} \end{aligned} \tag{8}$$

where c_1 is the ratio of peak heights of a spin-orbit pair in the spectrum of a standard compound, X_{SOS} is the spin-orbit splitting energy, and c_2 is the ratio of FWHMs in the standard spectrum of a standard compound. Coupling the variables in (8) allows a pair of spin-orbit peaks of an atom type to be fit with only three variables. If coupling is not desired, each spin-orbit peak can be entered as a separate atom type.

Provision is also made to keep the contributions from

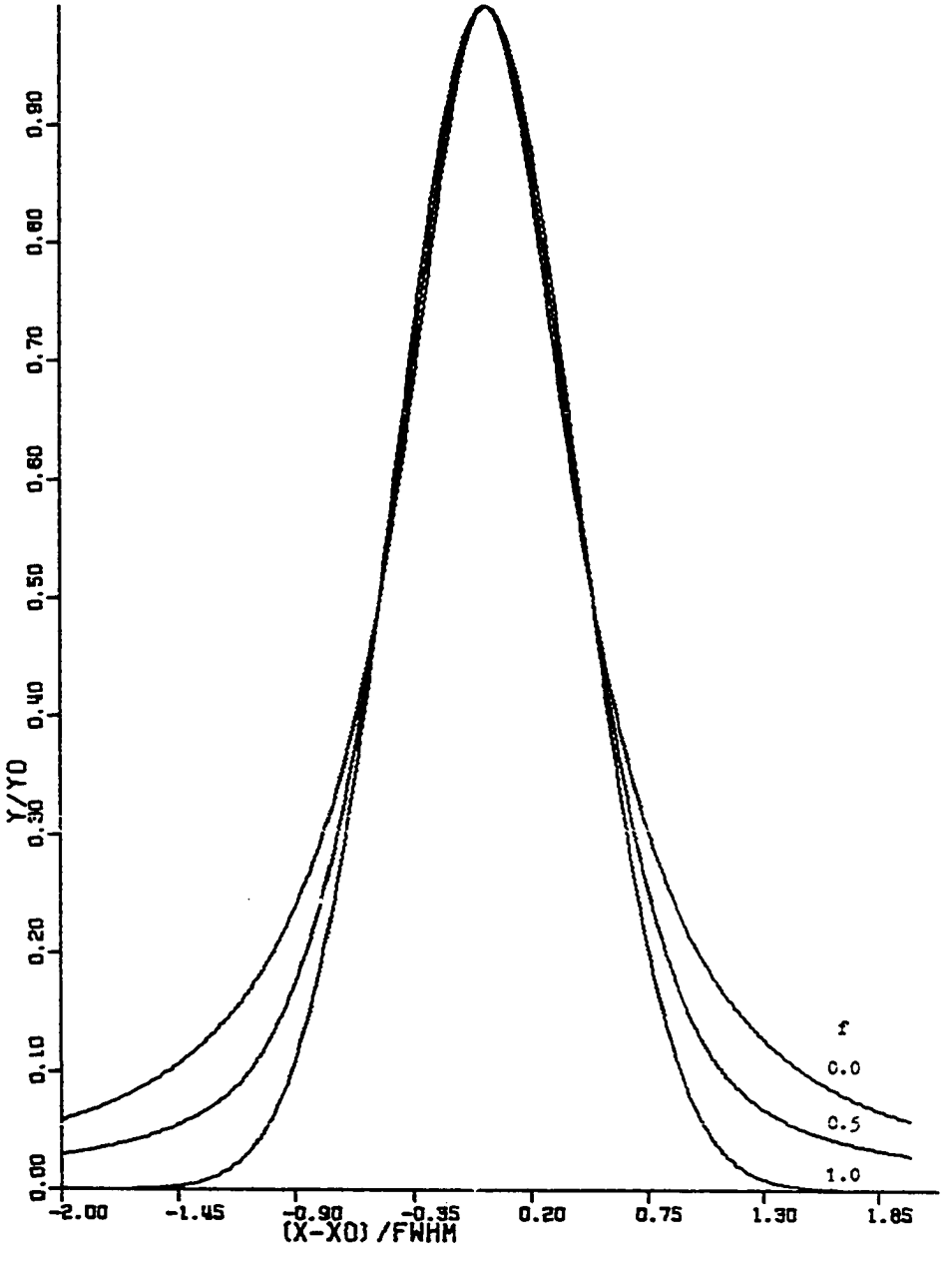

Figure 19. The fitting function used by APES

each atom type in a fixed ratio

$$Y_{CALC}(I) = \sum_{a=1}^{NNEQ} R_a Y_a(I) \qquad 0 \leq R_a \leq 1 \qquad (9)$$

where R_a represents the known (or suspected) relative ratio of type a atoms to the first atom (a=1). For example, the six terminal and two bridging chlorines in $Cs_3Mo_2Cl_8H$ would give rise to $R_1 = 1.000$ and $R_2 = 0.333$.

The user must input a series of control cards indicating how the fit is to be done. Included are the number of non-equivalent atoms suspected of giving rise to the spectrum, as well as their approximate heights, FWHMs and positions. Using these values a synthetic spectrum is calculated and refined. χ^2 is printed after each least squares cycle. Also printed are the refined values of the height, FWHM, and position, as well as their estimated standard deviations.[113] After convergence has been reached, the computed ratio of non-equivalent atoms (as computed from their relative areas) is printed. Next, a listing by channel number (the first channel corresponds to the first datum) of energy, raw data, smoothed data, baseline adjusted data, inelastic scattering corrected data, and calculated spectrum is made.

Finally, three plots are produced by APES through SIMPLOTTER.[114] The first plot has four curves: the raw data points (as "+" symbols), the smoothed curve, a curve for baseline corrected data, and a curve for the inelastic

scattering corrected data. The second plot has the corrected data points plotted and a curve for the synthetic spectrum. If there are two or more non-equivalent atoms, a third plot showing the corrected data points and the individual contribution of each non-equivalent atom will be shown.

When the program gives a reasonable match between the observed and calculated spectra, it is the third plot which represents the chemical information most clearly. The information of this plot will give insight into the relative number of non-equivalent atoms and will tell something about their oxidation state. From this, structural information can sometimes be derived. The program APES has been used successfully to determine structures of some compounds and seems to have wide applicability.

REFERENCES

1. Vahrenkamp, H. Angew. Chem. Int. Ed. Engl. 1978, 17, 379.

2. McCarley, R. E. In "Mixed Valence Compounds"; Brown, D. E., Ed.; Dreidel Publishing Company: Dordrecht, Holland, 1980; p 337.

3. Cotton, F. A.; Wilkinson, G. In "Advanced Inorganic Chemistry", 4th ed.; John Wiley and Sons: New York, 1980.

4. Cotton, F. A.; Koch, S. A.; Millar, M. Inorg. Chem. 1978, 17, 2084.

5. Calabrese, J. C.; Dahl, L. F.; Chini, P.; Longoni, G.; Martinego, S. J. Am. Chem. Soc. 1974, 96, 2614.

6. Muetterties, E. L. Angew. Chem. Int. Ed. Engl. 1978, 17, 545.

7. Muetterties, E. L.; Rhodin, T. N.; Band, E.; Brucker, C. F.; Pretzer, W. R. Chem. Rev. 1979, 79, 91.

8. Moskovits, M. Acc. Chem. Res. 1979, 12, 229.

9. Shustorovich, E.; Baetzold, R. C. J. Am. Chem. Soc. 1980, 102, 5989.

10. Yvon, K. In "Current Topics in Materials Science"; Kaldis, E., Ed.; North-Holland: New York, 1978; Vol. 3, Chapter 2.

11. Fischer, Ø. Appl. Phys. 1978, 16, 1.

12. Delgass, W. N.; Haller, G. L.; Kellerman, R.; Lunsford, J. H. "Spectroscopy in Heterogeneous Catalysis"; Academic Press: New York, 1979.

13. Czanderna, A. W., Ed. "Methods of Surface Analysis"; Elsevier Scientific Publishing Company: Amsterdam, 1975.

14. Johnson, K. H. Annu. Rev. Phys. Chem. 1975, 26, 39.

15. Shaik, S.; Hoffmann, R.; Fisel, C.; Summerville, R. J. Am. Chem. Soc. 1980, 102, 4555.

16. Cotton, F. A. Acc. Chem. Res. 1978, 11, 225.

17. Cotton, F. A.; et al. Science 1964, 145, 1305.

18. Kuznetzov, B. G.; Koz'min, P. A. Zhur. Strukt. Khim. 1963, 4, 55.

19. Cotton, F. A.; Harris, C. B. Inorg. Chem. 1965, 4, 330.

20. Cotton, F. A.; Curtis, N. F.; Johnson, B. F. G.; Robinson, W. R. Inorg. Chem. 1965, 4, 326.

21. Cotton, F. A. Chem. Soc. Rev. 1975, 4, 27.

22. Chisholm, M. H.; Cotton, F. A. Acc. Chem. Res. 1978, 11, 356.

23. Templeton, J. L. Prog. Inorg. Chem. 1979, 26, 211.

24. Klotzbucher, W.; Ozin, G. A. Inorg. Chem. 1977, 16, 984.

25. Norman, J. G., Jr.; Kolari, H. J.; Gray, H. B.; Trogler, W. C. Inorg. Chem. 1977, 16, 987.

26. Efremov, Y. M.; Samoilova, A. N.; Kozhukhovsky, V. B.; Gurvich, L. V. J. Mol. Spectrosc. 1978, 73, 430.

27. Bursten, B. E.; Cotton, F. A.; Hall, M. B. J. Am. Chem. Soc. 1980, 102, 6348.

28. Cotton, F. A.; DeBoer, B. G.; LaPrade, M. D.; Pipal, J. R.; Ucko, D. A. J. Am. Chem. Soc. 1970, 92, 2926.

29. Cotton, F. A.; Stanley, G. G. Inorg. Chem. 1977, 16, 2668.

30. Cotton, F. A.; Ilsley, W. H.; Kaim, W. J. Am. Chem. Soc. 1980, 102, 3464.

31. Garner, C. D.; Hillier, I. H.; Guest, M. F.; Green, J. C.; Coleman, A. W. Chem. Phys. Lett. 1976, 41, 91.

32. Cotton, F. A.; Extine, M. W.; Rice, G. W. Inorg. Chem. 1978, 17, 176.

33. Stephenson, T.; Bannister, E.; Wilkinson, G. J. Chem.

Soc. 1964, 2538.

34. McCarley, R. E.; Templeton, J. L.; Colburn, T. J.; Katovic, V.; Hoxmeier, R. J. In "Inorganic Compounds With Unusual Properties"; King, R. B., Ed.; American Chemical Society: Washington, D.C., 1976; Chapter 27.

35. Collins, D. M.; Cotton, F. A.; Koch, S.; Millar, M.; Murillo, C. A. J. Am. Chem. Soc. 1977, 99, 1259.

36. Sharp, P. R.; Schrock, R. P. J. Am. Chem. Soc. 1980, 102, 1430.

37. Katovic, V.; McCarley, R. E. Inorg. Chem. 1978, 17, 1268.

38. Katovic, V.; McCarley, R. E. J. Am. Chem. Soc. 1978, 100, 5586.

39. Bennett, M. J.; Brencic, J. V.; Cotton, F. A. Inorg. Chem. 1969, 8, 1060.

40. Cotton, F. A.; Kalbacher, B. J. Inorg. Chem. 1976, 15, 522.

41. Katovic, V. Ames Laboratory, Iowa State University; private communication, 1977.

42. San Filippo, J., Jr.; Sniodoch, H. J.; Grayson, R. L. Inorg. Chem. 1974, 13, 2121.

43. Jolly, W. L. "The Synthesis and Characterization of Inorganic Compounds"; Prentice Hall: Englewood Cliffs, 1970; Chapter 5.

44. Elwell, W. T.; Wood, D. F. "Analytical Chemistry of Molybdenum and Tungsten"; Pergamon Press: New York, 1971.

45. Ryan, L. M.; Taylor, R. E.; Paff, A. J.; Gerstein, B. C. J. Chem. Phys. 1980, 72, 508.

46. Luly, M. H. "APES: A Fortran Program to Analyze Photoelectron Spectra"; IS - 4694, Ames Laboratory: Ames, Iowa, 1979.

47. Cotton, F. A.; Ilsley, W. H.; Kaim, W. J. Am. Chem. Soc. 1980, 102, 1918.

48. Sachs, M. "Solid State Theory"; Dover: New York, 1974; Chapter 1.

49. Alexander, L. E. "X-Ray Diffraction Methods in Polymer Science"; Wiley-Interscience: New York, 1969; Chapter 1.

50. Gill, N. S.; Nuttall, R. H.; Scaife, D. E.; Sharp, D. W. A. J. Inorg. Nucl. Chem. 1961, 18, 79.

51. Popov, A. I.; Marshall, J. C.; Stute, F. B.; Person, W. B. J. Am. Chem. Soc. 1961, 83, 3586.

52. Walton, R. A. Coord. Chem. Rev. 1976, 21, 63.

53. Walton, R. A. J. Less-Common Met. 1977, 54, 71.

54. Chaudhari, P.; Giessen, B. C.; Turnbull, D. Scientific American April, 1980, 242, 98.

55. Geballe, T. H.; Hulm, J. K. Scientific American November, 1980, 243, 138.

56. Gorter, C. J. Rev. Mod. Phys. 1964, 36, 1.

57. de Haas, W. J.; Voogd, J. Leiden Commun. No. 199C 1929.

58. de Haas, W. J.; Voogd, J. Leiden Commun. No. 214B 1931.

59. Kittel, C. "Introduction to Solid State Physics", 5th ed.; John Wiley & Sons, Inc.: New York, 1976; Chapter 12.

60. Hulm, J. K.; Matthias, B. T. Science 1980, 208, 881.

61. Odermatt, R.; Fischer, Ø.; Jones, H.; Bongi, G. J. Phys. C. 1974, 7, L13.

62. Fischer, Ø.; Jones, H.; Bongi, G.; Sergent, M.; Chevrel, R. J. Phys. C. 1974, 7, L450.

63. Alekseevskii, N. E.; Glinski, M.; Dobrovolskii, N. M.; Tsebro, V. I. JETP Lett. 1976, 23, 412.

64. Decroux, M.; Fischer, Ø.; Chevrel, R. Cryogenics 1977, 17, 291.

65. Luhman, T. S.; Dew-Hughes, D. J. Appl. Phys. 1978, 49, 936.

66. Alterovitz, S. A.; Woollam, J. A.; Kammerdiner, L.; Luo, H. L. Appl. Phys. Lett. 1978, 33, 264.

67. Espelund, A. Acta Chem. Scand. 1967, 21, 839.

68. Opalovskii, A. A.; Fedorov, V. E. Izv. Akad. Nauk SSSR Neorg. Mater. 1966, 2, 443.

69. Chevrel, R.; Sergent, M.; Prigent, J. J. Solid State Chem. 1971, 3, 515.

70. Chevrel, R.; Sergent, M.; Prigent, J. Mat. Res. Bull. 1974, 9, 1487.

71. Perrin, A.; Chevrel, R.; Sergent, M. J. Solid State Chem. 1980, 33, 43.

72. Umarji, A. M.; Rao, G. V.; Sankaranarayanan, V.; Rangarajan, G.; Srinivasan, R. Mat. Res. Bull. 1980, 15, 1025.

73. Sergent, M.; Fischer, Ø.; Decroux, M.; Perrin, C.; Chevrel, R. J. Solid State Chem. 1977, 22, 87.

74. Delk, F. S. II; Sienko, M. J. Inorg. Chem. 1980, 19, 1352.

75. Yvon, K.; Paoli, A.; Flukiger, R.; Chevrel, R. Acta Cryst. 1977, B33, 3066.

76. Yvon, K.; Baillif, R.; Flukiger, R. Acta Cryst. 1979, B35, 2859.

77. Yvon, K.; Chevrel, R.; Sergent, M. Acta Cryst. 1980, B36, 685.

78. Cotton, F. A.; Haas, T. E. Inorg. Chem. 1964, 3, 10.

79. Guggenberger, L. J.; Sleight, A. W. Inorg. Chem. 1969, 8, 2041.

80. Mattheiss, L. F.; Fong, C. Y. Phys. Rev. B 1977, 15, 1760.

81. Bullett, D. W. Phys. Rev. Lett. 1977, 39, 664.

82. Andersen, O. K.; Klose, W.; Nohl, H. Phys. Rev. B 1978, 17, 1209.

83. Jarlborg, T.; Freeman, A. J. Phys. Rev. Lett. 1980, 44,

178.

84. Umarji, A. M.; Rao, G. V. Subba; Janawadkar, M. P.; Radhakrishnan, T. S. J. Phys. Chem. Solids 1980, 41, 421.

85. Schollhorn, R.; Kumpers, M.; Besenhard, J. O. Mat. Res. Bull. 1977, 12, 781.

86. Sheldon, J. C. Nature 1959, 4694, 1210.

87. Sheldon, J. C. J. Chem. Soc. 1960, 1007.

88. Cotton, F. A.; Curtis, N. F. Inorg. Chem. 1965, 4, 241.

89. Carmichael, W. M.; Edwards, D. A. J. Inorg. Nucl. Chem. 1967, 29, 1535.

90. Fergusson, J. E.; Robinson, B. H.; Wilkins, C. J. J. Chem. Soc. (A) 1967, 486.

91. Nannelli, P.; Block, B. P. Inorg. Chem. 1968, 7, 2423.

92. Nannelli, P.; Block, B. P. Inorg. Chem. 1969, 8, 1767.

93. Weissenhorn, R. G. Z. Anorg. Allg. Chem. 1976, 426, 159.

94. Wudl, F.; Nalewajek, D. Bell Laboratories, Murray Hill, New Jersey; private communication, 1980.

95. Sheldon, J. C. J. Chem. Soc. 1962, 410.

96. Baumann, H.; Plautz, H.; Schafer, H. J. Less-Common Met. 1971, 24, 301.

97. Lesaar, H.; Schafer, H. Z. Anorg. Allg. Chem. 1971, 385, 65.

98. Michel, J. B. Ph.D. Dissertation, Iowa State University, 1979.

99. Dorman, W. C.; McCarley, R. E. Inorg. Chem. 1974, 13, 491.

100. Brauer, G. "Handbuch der Praparativen Anorganischen Chemie", 2nd ed.; Ferdinand Enke: Stuttgart, 1960, p 325.

101. Clark, C. M.; Smith, D. K.; Johnson, G. J. "A Fortran

IV Program for Calculating X-Ray Powder Diffraction Patterns (Version 5)"; Department of Geosciences, Pennsylvania State University, 1973.

102. Hollander, J. M.; Jolly, W. L. Acc. Chem. Res. 1970, 3, 193.

103. Best, S. A.; Walton, R. A. Inorg. Chem. 1979, 18, 484.

104. Jellinek, F.; Pollak, P.; Shafer, M. Mat. Res. Bull. 1974, 9, 845.

105. Hamer, A. D.; Walton, R. A. Inorg. Chem. 1974, 13, 1446.

106. Cahen, D.; Lester, J. E. Chem. Phys. Lett. 1973, 18, 108.

107. Bancroft, G. M.; et al. Anal. Chem. 1975, 47, 586.

108. Betteridge, D.; et al. Z. Anal. Chem. 1973, 363, 286.

109. Shirley, D. A. Phys. Rev. B 1972, 5, 4709.

110. Subprogram CURFIT, as well as FCHISQ, MATINV, and FDERIV are used. Bevington, P. R. "Data Reduction and Error Analysis for the Physical Sciences"; McGraw-Hill Inc.: New York, 1969.

111. Marquardt, D. W. J. Soc. Ind. Appl. Math. 1963, 11, 431.

112. Fraser, R.; Suzuki, E. Anal. Chem. 1969, 41, 37.

113. The estimated standard deviations are based solely on counting statistics assuming each raw datum has a standard deviation of (number of counts)$^{\frac{1}{2}}$ and are probably underestimated. It is also assumed the binding energies are known exactly.

114. Scranton, D.; Manchester, E. "The Use of SIMPLOTTER, a High Level Plotting System"; Iowa State Computer Center: Ames, Iowa, March 1978.

ACKNOWLEDGEMENTS

As my formal education draws to a close I would like to thank my parents for their continual love and interest in my pursuits. The attainment of my goals would not have been possible without their formative influence.

I wish to thank my research advisor, Professor Robert E. McCarley, for the opportunity to work with him. His guidance and encouragement were particularly helpful during the more frustrating moments of this work.

I also wish to thank the members of Dr. McCarley's research group, past and present, for their assistance, helpful discussions and companionship. Special thanks are due to Dr. John B. Michel and William Beers.

My deepest appreciation goes to my wife, Jeanne, whose love and patience have been infinite.